DISSIPATION OF WAVES OVER A SALT MARSH MEADOW

J.O. KOETSIER

BACHELOR THESIS

Supervisors:
Dipl.-Ing. Matthias Kudella (Forschunszentrum Küste)
Dr. Ir. Jan S. Ribberink (University of Twente)
Period: 20-04-2015 until 01-07-2015
Faculty of Engineering Technology
Civil Engineering
Ede, 01-07-2015

UNIVERSITY OF TWENTE.

ABSTRACT

With an increasing awareness of ecological value and rising sea levels the use of vegetation in flood protection becomes widely accepted. To evaluate and quantify the benefits of a salt marsh meadow for flood protection, knowledge about the evolution of wave dissipation over the marsh is necessary. The objective of this research is to provide an empirical model which describes the development of wave dissipation over a salt marsh meadow under storm surge conditions. A method for the analysis of the data and the preparation of the model is also provided. The data is gathered in a large wave flume (Grosser Wellenkanal) in Hannover. A vegetated section of 39.44 meter length was built up of field excavated pieces of salt marsh turf. *Elymus, Atriplex,* and *Puccinnellia* are used as vegetation to represent a southern North Sea mars community. The data is obtained using 5 groups of 3 pressure transmitters and one group of 2 pressure transmitters. The pressure data is processed into surface elevation using linear wave theory. The surface elevation is calculated in frequency domain. It was necessary to use a low pass filter as the model was not appropriate for the higher frequencies. A high pass filter is applied to remove the offset of several spectrums. The method is limited as the pressure transmitters could not measure a signal of a wave with an amplitude of 0.1 meter. Several nonlinear tests were also excluded from the analysis. Nonlinear waves typically show more amplitude peaks in frequency domain. These peaks are determining for the wave shape in time domain. Some of the wave conditions showed peaks beyond the low pass filter.

Both an analysis of the evolution of wave height dissipation as well as an analysis of the wave energy flux dissipation is considered. A time interval with no influence of reflected waves is used in which the mean wave height is calculated. As theory states that wave dissipation shows an exponential behaviour, exponential functions are fitted to the mean wave height. The average wave energy flux is calculated using the mean wave height. Exponential functions are also fitted to this average wave energy flux plotted against the distance into the marsh. Empirical functions are derived on the basis of the parameters of the fitted functions. Both approaches showed low coefficients of variation but the approach on the basis of wave height dissipation seemed most accurate. Both approaches are presented as a function of the initial value and a decrease parameter. As a suggestion, the decrease parameter is presented as a function of the water depth. A comparison of the empirical functions with corresponding data from tests with mowed vegetation shows a significant faster process of dissipation for the derived empirical functions.

The salt marsh has a significant influence on wave height dissipation. This conclusion is supported by Möller et al. (2014) as they concluded that up 60% of wave height attenuation can be attributed to the vegetation. They used the same data for this conclusion. The evolution of wave dissipation shows a process that can be described as a function of the length of the salt marsh. This empirical relationship can be used as a quantitative basis for decisions concerning flood protection measurements. The present research showed a significant faster process of energy dissipation over a lower water depth. Recommendations include a further research to the dependency of the decrease parameter on other parameters than the water depth. Further research to the influence of the water depth on the dissipation process seems also necessary as the present research is only based on two water depths. Further research with the use of a longer salt marsh will benefit the quality of the results as the present data only seemed to describe the first section of the process of wave dissipation.

PREFACE

This thesis is the final report I make for my bachelor Civil Engineering at the University of Twente. I did my thesis at the Forschungszentrum Küste (FZK) in Hannover. I had a great time there because of the relaxed atmosphere and especially because of the excellent supervision. I therefore learned a lot of new theory and skills. For me it was great to finally do a research instead of learning theory and making exams.

I therefore especially want to thank Matthias Kudella for his help and time. Matthias was my supervisor during my internship and I could always ask him for help. I also want to thank Stefan Schimmels for his effort in finding a research topic, arranging everything for my internship and for this valuable feedback and explanations of wave theory. I also want to thank my supervisor from the University of Twente, Jan Ribberink for introducing me to Stefan Schimmels and for his valuable feedback. The feedback I got from Matthias, Stefan and Jan Ribberink improved my report significantly.

I will not forget to thank all of my 'colleagues' at the FZK, especially my 'office-mate' Gholamreza Shiravani with whom I have had a lot of conversations about a wide range of topics. I also want to thank Gholamreza for his feedback on my report. Lastly I want to thank my roommates in Hannover for the great time I had.

Otto Koetsier
Ede, 01-07-2015

TABLE OF CONTENTS

LIST OF FIGURES

LIST OF TABLES

LIST OF PARAMETERS

h = water depth above marsh surface (m)
H = generated wave height (m)
H_{mean} = mean wave height on a certain interval (m)
H_0 = initial wave height (m), (measured at PT 2.3)
η = surface elevation (m)
d = depth of pressure transmitter (m)
T = wave period (s)
λ = wavelength (m)
p = total pressure (Pa)
p_D = dynamic pressure (Pa)
ρ = density of liquid ($kg \cdot m^{-3}$)
g = standard acceleration due to gravity ($m \cdot s^{-2}$)
K_p = pressure response factor (-)
k = wavenumber (m^{-1})
ω = angular frequency (rad/s)
f = frequency (Hz)
C_g = group velocity (m/s)
b_P = decrease parameter corresponding to the empirical formula describing the wave energy flux dissipation (m^{-1})
b_H = decrease parameter corresponding to the empirical formula describing the wave height dissipation (m^{-1})
P = energy flux (W/m)
P_0 = initial energy flux (W/m) (calculated from the signal of PT 2.3)
E = mean wave energy density per unit of horizontal area ($J \cdot m^{-2}$)
$L_{decrease}$ = decrease length (m)

a.

b.

Figure 1| Photographs of the experiments. a, generated waves in the flume. **b,** vegetation inside the flume.

1. INTRODUCTION

1.1. RESEARCH MOTIVATION

The climate is changing and rising sea levels, increasing storminess and land subsidence cause an increasing risk from flooding (Gedan et al., 2010; Temmerman, De Vries & Bouma, 2012; Möller et al., 2014). More than one third of the world's population lives in coastal areas and small islands (UNEP 2006 in Gedan et al., 2010). Therefore flood protection becomes increasingly important. Salt marshes attenuate waves and, as a result, provide coastal protection (Möller et al., 2006; Koch et al., 2009: Bouma et al., 2010; Gedan et al., 2011; Möller et al., 2014). The plants directly attenuate waves through the energy dissipation caused by their physical structure (Fonseca & Cahalan, 1992; Moller et al., 1999; Mendez & Losada 2003, Koch et al. 2009). They also stabilize and build up sediment (Fonseca et al., 1981; Fonseca & Cahalan, 1992; King & Lester, 1995; Boorman, 1999; Möller, 2006; Koch et al., 2009; Bouma et al., 2010; Gedan et al., 2011). Therefore salt marshes are now widely recognised for their economic value (Boorman 1999). However, a degradation and loss of tidal marshes is noticed (Gedan et al., 2010; Temmerman et al., 2012). Many coastal managers prefer structural engineering approaches as they provide the easiest and most dependable protection from flooding. Salt marshes can attenuate waves before they reach the coast. Structural engineering solutions tend to destroy natural habitat. Salt marshes combine ecosystem services and coastal protection (Koch et al., 2009). Salt marshes therefore eminently meet the definition of the new 'Building with Nature' principle.

Many researches have concluded a significant influence of salt marshes in wave attenuation (Fonseca & Cahalan, 1992; Möller et al., 1996; 1999; 2001; 2006; Bouma et al., 2010; Paul & Amos, 2011) however the effect of wave height attenuation during storm surge conditions, when flood protection is most important, is only investigated in Möller et al. (2014). They concluded that up to 60% of wave height attenuation can be attributed to the salt marsh. Möller et al. (2014), however, did not investigate the evolution of wave dissipation over the marsh. A better understanding of the evolution of wave dissipation is necessary in order to quantify the benefits of the marsh. This knowledge will provide a relationship which can be used for further research with different salt marshes. Eventually a relationship will be derived which is applicable for all salt marsh conditions. This relationship can be used as a quantitative basis for decisions concerning ecosystem engineering.

As no research has yet been executed on the evolution of extreme wave dissipation over salt marshes (Möller et al., 2014) a method has not yet been developed. The data for the present research is gathered in a large wave flume (Möller et al., 2013). To make this method also applicable for field research the data is gathered using pressure transmitters.

The present research is hereby an extension of the research of Möller et al. (2014). The test data for the present research is gathered as described in Möller et al. (2013) which is part of *Hydralab IV*. For this thesis, the tests were already conducted. The tests were conducted in a 300 meter long wave flume, the Grosser Wellenkanal (GWK) in Hannover (see Figure 1). *Elymus, Atriplex,* and *Puccinnellia* are used as vegetation to represent a southern North Sea mars community (Möller et al., 2014).

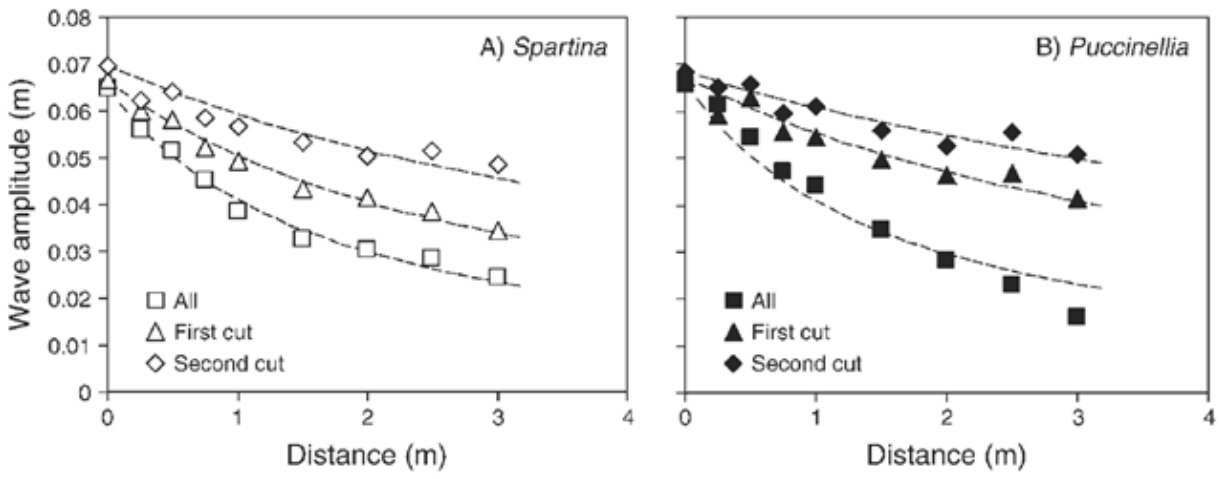

Figure 2| Expected shape of wave attenuation visualized by plotting the wave amplitude (Bouma et al., 2010)

1.2. Research Objective

The main objective is to provide an empirical relationship which describes the evolution of wave dissipation over a salt marsh under extreme conditions. As no research has yet been executed on the evolution of extreme wave dissipation over salt marshes (Möller et al., 2014) a method has not yet been developed. The second objective of this research is therefore to develop a method and to investigate the limits of this method. As the data is gathered using pressure transmitters (Möller et al., 2013) the method will be based on this data source.

The difference between the present study and former studies is that the present study will focus on extreme conditions. This is important because it will benefit to the knowledge about flood protection using vegetation. Möller et al. (2014) focussed on the amount of wave dissipation over the salt marsh. The present research will focus on the development of wave dissipation. For both the present research and the research of Möller et al. (2014) the same test data is used. The tests were carried out as a part of Hydralab IV (Möller et al., 2013).

1.3. Research Questions

The research questions are directly related to the research objective. The first three questions concern the transformation from the pressure signal into surface elevation. Both an approach on the wave height dissipation as an approach on the basis of the wave energy flux dissipation is considered. An approach on the basis of wave height dissipation is considered as this directly originates from the calculated surface elevation. An approach on the basis of the wave energy flux is considered as this includes more parameters.

Q1: Which approach could serve as a method for the transformation from the pressure signal into surface elevation?
Q2: What are the limits of this approach?
Q3: What is the uncertainty in the calculated surface elevation (from the pressure signal) compared to the signal of the wave gauges?
Q4: Which function could represent the relationship between the average wave height and the distance into the marsh? What is the uncertainty in this function?
Q5: Which function could represent the relationship between the average wave energy flux and the distance into the marsh? What is the uncertainty in this function?
Q6: Which parameters influence the evolution of wave dissipation?
Q7: Which of the approaches as presented in Q4 and Q5 shows the least uncertainty?
Q8: What is the influence of the vegetation on wave dissipation?

1.4. Hypothesis

The hypothesis is discussed per research question:

Q1: As linear wave theory is able to provide a relationship between pressure and surface elevation it is expected to be a good approach for the transformation of the pressure signal into surface elevation.
Q2: Not all waves have a linear behaviour. The limits of this method are expected to be at the nonlinear waves. Other limits of the method are expected to be at the pressure signal. The pressure transmitters cannot measure a signal at a certain water depth – wave height relation. This depends on the calibration of the devices.
Q3: The uncertainty is expected to increase with increasing nonlinearity.
Q4 and Q5: As previous studies found exponential wave decay with distance into the vegetation (Paul & Amos, 2011; Möller et al., 1999; Bouma et al., 2010), this is also expected in the present study (see Figure 2).
Q6: The parameters of the empirical functions are expected to be dependent on the initial wave height, wave period and water depth. Möller et al. (1996) has concluded that reduction in wave energy and wave height is strongly related to water depth. As linear wave theory

includes both wave height and wave period these parameters are also likely to determine the evolution of dissipation.
Q7: As the wave energy flux includes wave period, water depth and wave height this is expected to show the least uncertainty.
Q8: As Möller et al. (2014) have concluded that the salt marsh has a significant influence on wave dissipation this is also expected in the evolution of wave dissipation.

1.5. METHODOLOGY

The methodology is presented on the basis of the research questions:

Q1: As the hypothesis states that linear wave theory is expected to be a good approach the first step is to provide the necessary equations. As the formulas require a calculation in frequency domain (see chapter 3) a fast Fourier transform (FFT) will be applied. After the calculation of the surface elevation in frequency domain, an inverse fast Fourier transform (IFFT) will be applied to obtain the surface elevation in time domain. For this the phase spectrum from the pressure signal is used.
Q2: The limits of the approach are expected to be at the nonlinear waves. Careful observation of the behaviour of the parameters of the formulas will be used in order to determine the limits. The limits at the waves with a low wave height are simply determined with the use of the pressure signal. If the pressure signal shows only noise the test should be excluded from the analysis.
Q3: The uncertainty will be calculated using the signal of the wave gauges. An optimal output of the calculations will deliver a surface elevation over time which is exactly the same as the signal of the wave gauge at the same x-position. The uncertainty is calculated using the coefficient of variation (see chapter 3).
Q4: The function is based on the relationship between the average wave height and the distance into the marsh. To derive this relation the average wave height will be calculated at every location of the pressure transmitters. For this a time frame is set in which the influence of reflected waves is excluded. A function is plotted using Matlabs fit function which is characterised by Pearson's correlation coefficient (appendix D). The uncertainty will be calculated using the coefficient of variation (appendix E). For this the calculated average wave height is plotted against the empirical average wave height at the same location.
Q5: The same approach as at research question four is used except that the average wave height is used to calculate the average wave energy flux.
Q6: Careful observation of the behaviour of the derived empirical functions and their parameters will answer this question.
Q7: A simple comparison between both uncertainties will deliver an answer on this question.
Q8: For this the same approach as used for the derivation of the empirical formulas is used. The empirical function corresponding to the tests without vegetation can then be compared with the empirical functions corresponding to wave attenuation over the salt marsh. The comparison will include a visual representation and a comparison on the basis of the parameters of the derived function.

1.6. OUTLINE

The report is organised as follows. First, the test set up at the GWK is described in chapter 2. This also includes a definition of the coordinate system and a table of all test runs. Secondly, the data processing is described in chapter 3. The model, in which the data is processed, is discussed as this model is one of the research objectives. This chapter includes a detailed explanation of the used equations, the low pass filter, the model uncertainty and the limits of this model. Thirdly, the data analysis is discussed in chapter 4. This chapter includes two approaches. First an approach on the basis of wave height dissipation is presented and secondly an approach on the basis of the wave energy flux dissipation is presented. Lastly, the report contains a discussion of the data and data processing (chapter 5) and the conclusions (chapter 6) and recommendations (chapter 7). Several appendices support this report by containing more detailed information.

2. TEST SET-UP

The description of the set-up in this chapter is a summary of relevant information derived from the data storage report presented by Möller et al. (2013). This data is part of Hydralab IV. The present research uses this data and therefore a description is given. Paragraph 2.1 contains general information. Paragraph 2.2 contains information about the coordinate system. Several figures and tables about the set-up, test runs and instrumentation support this chapter.

2.1. GENERAL DESCRIPTION

A vegetated test section of 39.44 meter length was built up of 204 cut (field excavated) pieces of saltmarsh turf of size 1.16 x 0.76 m each. *Elymus, Atriplex,* and *Puccinnellia* are used as vegetation to represent a southern North Sea mars community. The 39.44 m long section was split in two sections. In the first (front) section the species plant turf elements were placed in parallel next to each other width-wise, for a distance of 5.8 m (i.e. five marsh blocks deep). This was done for a more detailed research of the drag forces of the species. It has a negligible influence on the test results that will be used to calculate the wave attenuation. Behind this front set of 6 x 5 marsh blocks, the remaining 174 pieces of turf were arranged in a chequer board pattern to simulate a mixed marsh community (figure 3).

At the front end of the platform with vegetation, a flat concrete block surface of 13 m length was built up to the level of the marsh surface. In front of this, a ramped concrete slope was built (slope of 1:10) for a distance of 7 m, in front of which the slope increased to 1:1.7 over a

distance of 1.2 m. The surface of the flat concrete section in front of the vegetation blocks was at 1.5 m above the flume base. The slope allowed the waves to shoal and/or break (depending on the generated wave conditions), as they would do in a natural shallow water marsh setting. The vegetated platform was raised to a height of +1.5 m above the base of the tank by constructing a 1.2 m high sand base on top of which a geotextile surface was placed with the marsh pieces placed onto the geotextile by crane. The elevated sand base was required because of the minimum usable water level of ca +2m within the GWK flume. To the front and the rear of the vegetated section, the concrete block level was raised so that the surface of the concrete was at the same level as the vegetated section surface (figure 3 and figure 4).

A small (ca. 45cm) gap remained between the vegetation blocks and the side of the flume on one (the North) side of the flume, as well as at the end of the vegetation section facing away from the wave generating system. The vegetation was transported in blocks. These blocks did not perfectly fit into the flume. Both these gaps were filled with very coarse gravel material, with a dividing vertically placed flexible plastic lining placed at the interface between the marsh blocks and the gravel. The concrete blocks in front of and behind the marsh surface, as well as the gravel bund on the South and far side of the flume allowed the marsh blocks to remain in position under the generated wave conditions. Sand movement into the vegetated test section was also successfully avoided. Conditions of 2 different water depths (1.0 and 2.0 m above the test section and seven wave heights (H: 0.1, 0.2, 0.3, 0.4, 0.6, 0.8, and 0.9m) were simulated for the present research (see Table 2). 17 pressure transmitters (referred to as PT) and 12 wave gauges (referred to as WG) were used for the analysis (see Table 1). Pressure transmitters measure a pressure signal over time; wave gauges measure the surface elevation over time. For each run, full wave spectra and wave parameters (height, period and steepness) were recorded. The duration of 1 run is 100 waves. Tests were conducted with intact and removed (mowed) vegetation, with the latter tests acting as control runs to determine the effect of the vegetation as opposed to the topographic effect of the platform. The entire vegetated test section was illuminated for the benefit of the plants, at least whenever these were emergent between experimental runs, by a total of 60 lamps (GE 750W 400V PSL or equivalent) mounted along the side of the flume. The readings of the transmitters were logged with one data acquisition system (DAQ). The DAQ took care of synchronisation and sampling operated at a frequency of 100 Hz. Pressure transmitters PT 2 EMC 2 and PT 2 EMC 3 are pressure transmitters at the location of installed Electromagnetic Current Meters (EMC) and therefore have a different name.

2.2. Coordinate System

The origin is positioned at the location of pressure transmitter PT 2.3. This is the last pressure transmitter in front of the marsh. The horizontal x-axis is positive in the direction of wave propagation towards the structure. The horizontal y-axis is positive along the wave board from the office-side of the board towards the far side (North wall). The vertical z-axis is positive upwards from the base of the flume. The test section structure remained the same in all test runs. The water depth was varied between 1.0 and 2.0 m above the surface of the vegetated test the section (i .e. between 2.5 and 3.5 m above the flume base) in individual test runs and was lowered to below the root zone of the vegetation (ca. 40 cm below the vegetated marsh surface) for the duration of at least 24 hours after each two days of submersion during the experiment.

Table 1| Location of instrumentation (PT=pressure transmitter, WG=wave gauge, PT EMC= pressure transmitter at the location of electromagnetic current meters)

Instrumentation	x(m)	y(m)	z(m)
PT & WG 2.1	-3.62	2.33	1.53
PT & WG 2.2	-1.55	2.77	1.53
PT & WG 2.3	0	2.33	1.53
PT 2 EMC 2	9.01	0.20	1.73
PT 3 EMC 3	11.67	0.84	1.74
PT 5.1	12.54	2.50	1.55
PT 5.2	14.61	2.50	1.48
PT 5.3	16.16	2.50	1.49
PT & WG 3.1	24.55	2.50	1.49
PT & WG 3.2	26.62	2.50	1.57
PT & WG 3.3	28.17	2.50	1.57
PT 6.1	34.54	2.50	1.44
PT 6.2	36.61	2.50	1.43
PT 6.3	38.16	2.50	1.46
PT & WG 4.1	45.68	2.45	1.53
PT & WG 4.2	47.75	2.45	1.54
PT & WG 4.3	49.3	2.45	1.55

3. Transformation of Pressure Signal into Surface Elevation

In this chapter the transformation of the pressure signal to surface elevation is discussed. The approach is based on linear wave theory. Paragraph 3.1 answers research question one ('*Which approach could serve as a method for the translation from the pressure signal into surface elevation?*'). In this paragraph the equations are discussed in an order as is used in the model. All calculations are done in frequency domain. Paragraph 3.2 contains a discussion about the application of an empirical correction factor which is applied in frequency domain.

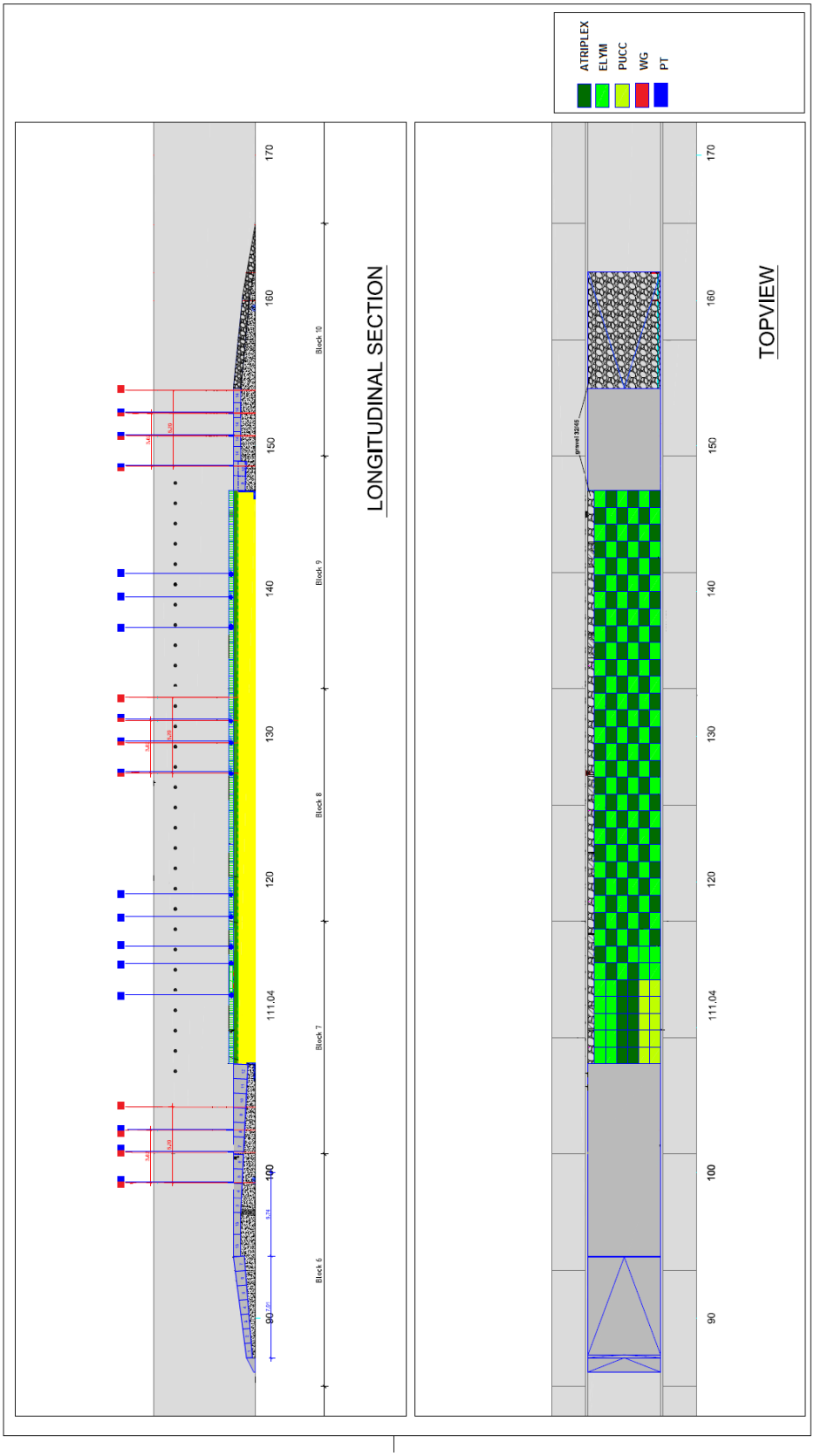

Figure 3| Experimental layout (Möller et al., 2013)

Table 2| Test runs

Date	code	h(m)	T(s)	H_g (m)	breaking/ nonbreaking
15-10-14	1502	2	1.5	0.1	nonbreaking
15-10-14	1504	2	2.1	0.2	nonbreaking
15-10-14	1506	2	2.9	0.2	nonbreaking
17-10-14	1702	2	2.9	0.2	nonbreaking
17-10-14	1703	2	2.5	0.3	nonbreaking
17-10-14	1705	2	3.6	0.3	nonbreaking
21-10-14	2102	2	2.9	0.4	nonbreaking
21-10-14	2105	2	4.1	0.4	nonbreaking
21-10-14	2107	2	3.6	0.6	nonbreaking
22-10-14	2205	2	5.1	0.6	nonbreaking
24-10-14	2402	2	4.1	0.8	transitional
24-10-14	2404	2	5.8	0.8	transitional
24-10-14	2407	2	4.4	0.9	transitional
25-10-14	2502	2	6.2	0.9	transitional
18-10-14	1803	1	2.1	0.2	nonbreaking
18-10-14	1805	1	2.9	0.2	nonbreaking
22-10-14	2207	1	2.9	0.4	transitional
25-10-14	2504	1	3.3	0.5	breaking
25-10-14	2506	1	4.6	0.5	breaking

Tests with mowed vegetation:

29-10-14	2902	2	2.9	0.4	nonbreaking
29-10-14	2905	2	4.1	0.4	nonbreaking
31-10-14	3110	2	3.6	0.6	nonbreaking
31-10-14	3112	2	4.1	0.8	transitional
31-10-14	3105	1	2.9	0.4	transitional

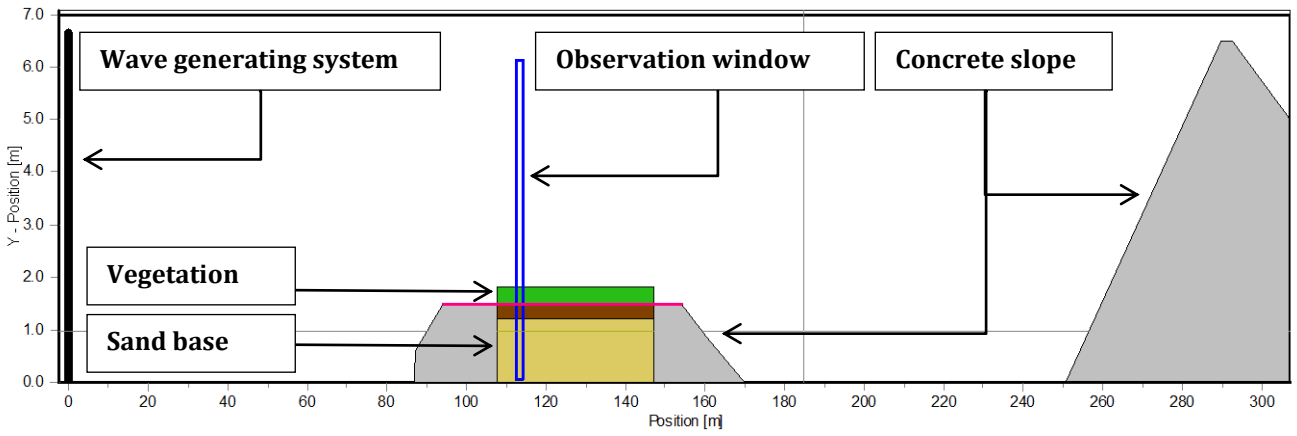

Figure 4| Experimental setup

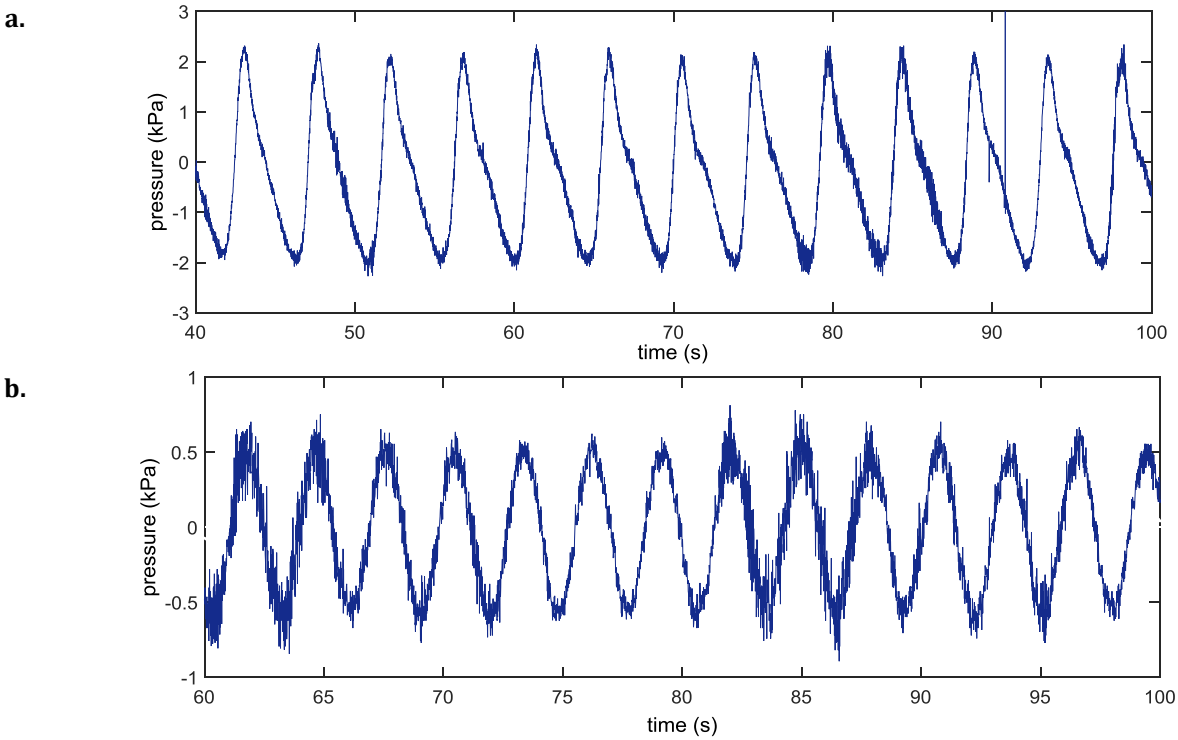

Figure 5| Signal from pressure transmitter. a, pressure signal of a nonlinear wave, signal from test 2506 and PT 2.1: H(m)=0.5, T(s)=4.6, h(m)=1. **b,** pressure signal of a linear wave, signal from test 1506 and PT 2.1: H(m)=0.2, T(s)=2.9, h(m)=2.

As in frequency domain, due to the behaviour of the pressure response factor, the surface elevation tends to infinite at a certain frequency a low pass filter is necessary. The derivation and application of this low pass filter is discussed in paragraph 3.3. Paragraph 3.4 contains information about excluded tests. The answer on research question two ('*What are the limits of this approach?*') is provided here. Paragraph 3.5 contains a discussion of the uncertainty in the calculated surface elevation. This uncertainty is calculated in time domain using a comparison of the surface elevation measured by the wave gauges at the same x-positions as the pressure transmitters. An answer on research question 3 is herewith provided ('*What is the uncertainty in the calculated surface elevation (from the pressure signal) compared to the signal of the wave gauges?*').

3.1. Model Structure

In order to analyse the data, the pressure signal from the pressure transmitters is translated into surface elevation. For this calculation a model is built based on linear wave theory. This paragraph contains a step by step explanation of the model. The formulas are derived from the book of Dean and Darymple (1984) and the report of Bishop and Donelan (1987).

Examples of the signal of the pressure transmitter are plotted in figure 5 a and b. The time interval in these figures is an interval without the influence of reflected waves based on the interval of Möller et al. (2014).

At first, this signal is translated into a signal in frequency domain using a fast Fourier transform (FFT), see figure 6 a and b. The figures show typical shapes of the signal of the pressure transmitter. Note that the frequencies higher as 1 Hertz include some noise components which are not displayed. Nonlinear waves (see figure 5a and figure 6a) typically show more peaks as, according to theory, they exist of more wave components (Dean & Darymple, 1984). Linear waves show one peak as they correspond to a sine wave.

The second step in the model is the calculation of the wavenumber (k) using the dispersion relation (eq. 1):

$$\omega^2 = gk\,tanh(hk) \qquad \text{eq. (1)}$$

Where

ω	= angular frequency (rad/s)
	($\omega = 2\pi/T$, T = wave period (s))
k	= wavenumber (m^{-1})
	($k = 2\pi/\lambda$, $\lambda =$ wavelength (m))
g	= standard acceleration due to gravity ($m \cdot s^{-2}$)
h	= water depth (m)

Considering this equation, the wavenumber is calculated using an iterative process. The wave number corresponding to deep water waves is used to start this process as this seems to be a good approximation:

$$\lambda = 1.56T^2 \qquad \text{eq. (2)}$$

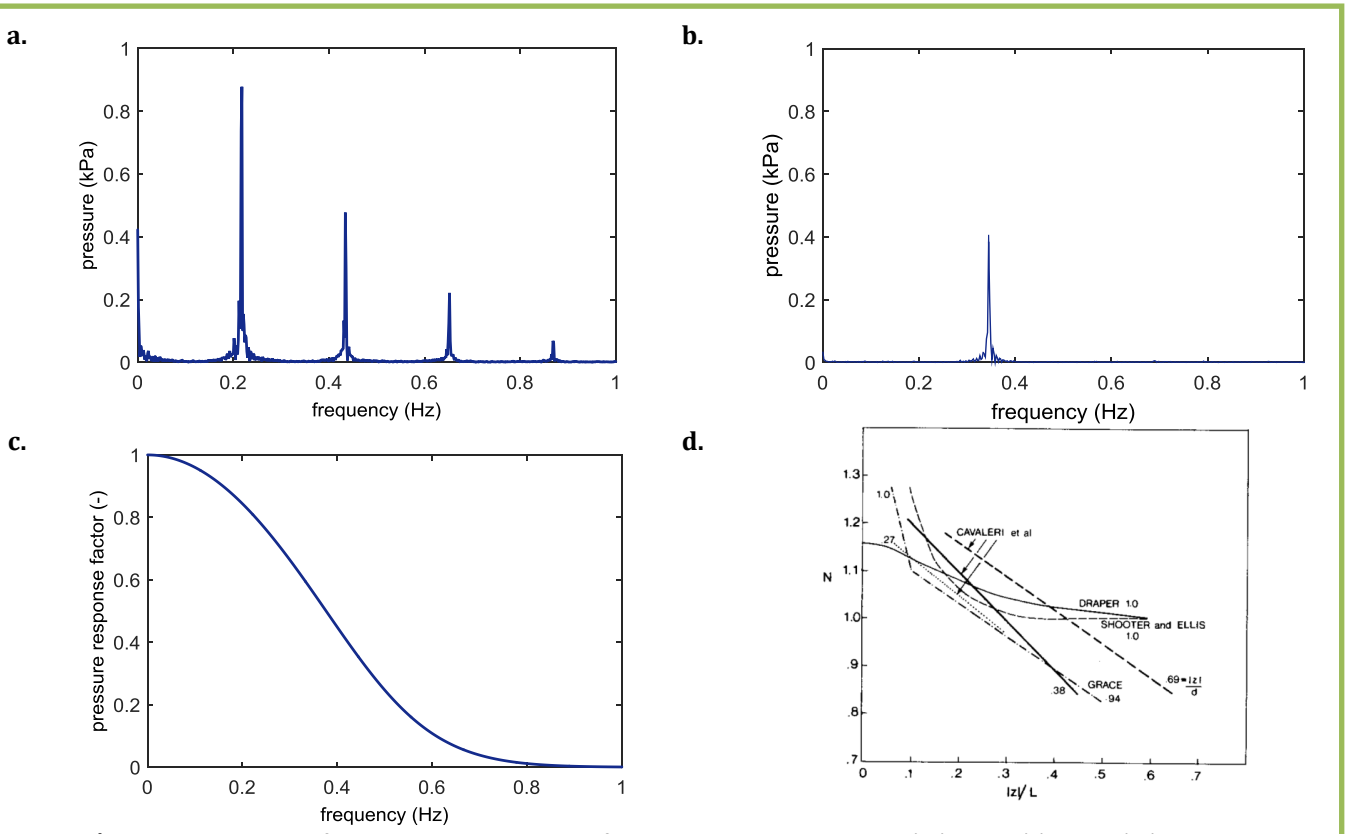

Figure 6| a, pressure signal of a nonlinear wave, signal from test 2506 and PT 2.1: H(m)=0.5, T(s)=4.6, h(m)=1. **b,** pressure signal of a linear wave, signal from test 1506 and PT 2.1: H(m)=0.2, T(s)=2.9, h(m)=2. **c,** correction factor plotted against the depth of the pressure transducer (z) divided by the wavelength (L) (Bishop & Donelan, 1987). **d,** typical shape of the evolution of the pressure response factor plotted against the frequency (example taken from test 1506, see figure 6b).

The third step is the calculation of the pressure response factor (K_p) at the depth of the pressure transmitters (d):

$$K_p(d) = \frac{\cosh(k(h-d))}{\cosh(kh)} \qquad \text{eq. (3)}$$

Where
d = depth of pressure transmitter (m)

Depending on the generated wave period of the test, the pressure response factor tends to 0 at a certain frequency (see figure 6c). The model treats every frequency in the spectrum as a free wave. As the frequency increases to a frequency of 50 Hz (due to noise) the wave period (according to the model) decreases down to 0.02 seconds. The corresponding wave number therefore increases to an order of magnitude of 10^4 and therefore the pressure response factor decreases to a value close to zero.

The fourth step is the calculation of the surface elevation at every frequency (including the noise components):

$$\eta = \frac{p}{\rho g K_p(d)} \qquad \text{eq. (4)}$$

Where
p = pressure (kPa)
ρ = density of liquid (1000 kg· m^{-3})

As the pressure response factor tends to zero; the surface elevation will tend to an infinite value. Therefore it is necessary to apply a low pass filter. The implementation of this filter is discussed in paragraph 3.3.

The last step is the transformation of the calculated surface elevation into time domain. This is done using an inverse fast Fourier transform (IFFT). The phase spectrum obtained when conducting the fast Fourier transform on the pressure series is used (the first step).

3.2. Empirical Correction Factor

According to Bishop and Donelan (1987) many researchers apply an empirical correction factor (N) to account for the differences between the theoretical surface elevation and observed surface elevation. The factor is applied in frequency domain (see eq. 5):

$$\eta_{corrected} = N \times \eta \qquad \text{eq. (5)}$$

The correction factor differs along investigations (see figure 6d). To find an appropriate function for the factor N, the signal from the pressure transmitter is compared with the signal from a wave gauge at the same x-position. The comparison is done in frequency domain. As an

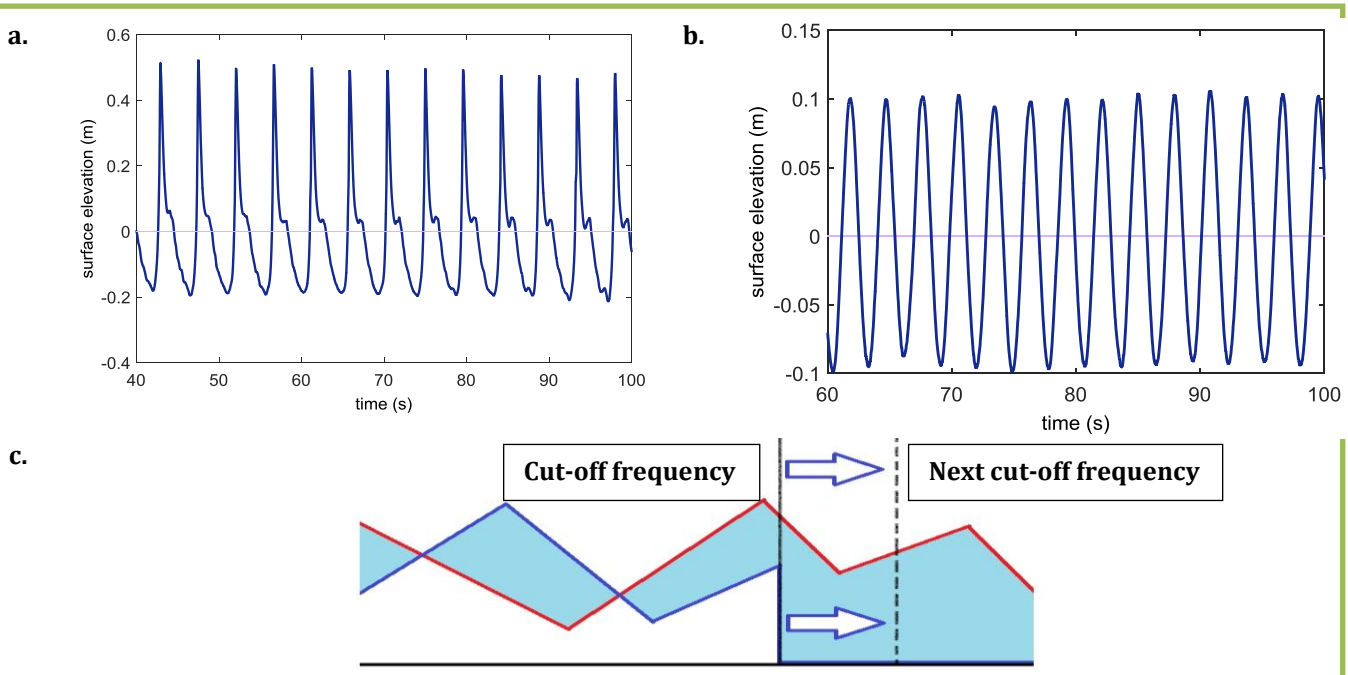

Figure 7| Surface elevation and low pass filter. a, wave gauge signal of a nonlinear wave, signal from test 2506 and WG 2.1: H(m)=0.5, T(s)=4.6, h(m)=1. **b,** wave gauge signal of a linear wave, signal from test 1506 and WG 2.1: H(m)=0.2, T(s)=2.9, h(m)=2. **c,** schematic figure of the process of determining the optimal location of the low pass filter. The blue and red lines represent the calculated and measured surface elevation in frequency domain. The light blue surface represents the sum of absolute differences.

underestimation is noticed but no clear relation can be derived, the factor is set to: N=1.0079. See Appendix C for the data. The factor is applied on the whole spectrum before transforming it into time domain. The signal in time domain is shown in figure 7a and b.

3.3. Low Pass Filter

As the pressure response factor decreases to a value close to zero (see figure 6c), the surface elevation increases up to an infinite value. Two methods are considered to avoid this problem. The first is to apply a low pass filter at the frequency where the surface elevation starts to increase to physically not relevant values. The frequency at which this behaviour occurs depends on the wave period and the water depth (see eq. 1, 3 and 4). Therefore a systematic approach based on both parameters is desirable. This cut-off frequency is derived with the use of the wave gauge signal. Three wave gauge pressure transmitter combinations were used for the calculation: PT2.1-WG2.1, PT3.3-WG3.3 and PT4.2-WG4.2. The criterion for these combinations is that they are installed at locations over the whole length of the platform.

To derive the optimal cut-off frequency first a high pass filter at a frequency of 0.01 Hertz is set to exclude the offset (see appendix B). An offset is caused by noise as the whole pressure signal is used for this calculation. Starting at this value a low pass filter is applied with steps of 0.01 Hertz (see figure 7c). Amplitudes corresponding to frequencies higher as the cut-off frequency are set to 0. Then, over all values in the spectrum, the absolute difference between the amplitude of the signal of the wave gauge and the calculated amplitude from the signal of the pressure transmitter is calculated. The summation of these values is attached to a cut-off frequency. This process is repeated up to a value of 1.5 Hertz, as at this frequency no physically correct behaviour was noticed by any of the tests. This results in 149 summated values for every test. For every test the cut-off frequency is defined as the value corresponding to the lowest sum of absolute differences.

Based on the results, for periods up to T(s)=2.9 and corresponding water depth of h(m)=2 a cut-off frequency of 0.08 Hertz plus the frequency corresponding to the wave period is derived (see Appendix A). Tests with periods higher than 2.9 seconds show a nonlinear behaviour and therefore the cut-off frequency lays higher (more peaks). As no relationship seems possible the minimum cut-off frequency is chosen for the calculations: 0.51 Hertz (see Appendix A). By using the minimum value none of the calculations would include wrong values of the surface elevation. The tests over a water depth of one meter also do not seem to show a relationship. Therefore also for these tests the minimum value of the optimal cut-off frequency is used for the calculations. This value is considerably higher than the value for the tests over a 2 meter water depth: 0.62 (see Appendix A). The low pass filter is applied after conducting the fast Fourier transform (first step in paragraph 3.1.) so that the calculation uses a faster process.

Due to the nonlinear shape of certain waves these waves show more than one amplitude peak in their spectrum (see figure 6a). These peaks are essential in determining the shape of the wave in time domain. Some peaks lay beyond the cut-off frequency and are therefore ignored when using the discussed approach. When analysing these results it would lead into wrong conclusions. The tests which show this behaviour are therefore excluded (see paragraph 3.4). To include these peaks in the calculations a different approach is considered. In this approach only the frequency corresponding to the wave period is used for the calculation. The surface elevation for the whole spectrum (up to 50 Hertz) is calculated using this approach and it therefore includes al amplitude peaks. Unfortunately, using this approach an underestimation is noticed at the peaks not corresponding to the peak at the wave period. This underestimation seems to increase with increasing wave height and wave period. It also seems to increase with frequency. As time is short this approach is not worked out in detail and is therefore not used in the further analysis.

3.4. Method Limits

An objective of the present research is to define a method for the derivation of the empirical model. Part of this method is given in this chapter. As discussed in paragraph 3.3, this method has certain limits. As a low pass filter is applied some frequency peaks may lie beyond the cut-off frequency and are therefore ignored. As these peaks are determining for the shape of the waves in time domain the tests in which this occurs have to be excluded. Careful observation leads to the conclusion that only some nonlinear waves show peaks beyond the cut-off frequency. For other tests, linear theory seems to be a good approximation as all the amplitude peaks lay before the cut-off frequency. After careful observation the tests listed in table 3 (under the dotted line) are excluded.

Another limit lies at low wave amplitudes. In the present research test 1502 is excluded because the pressure transmitter did not deliver a signal. The wave height of 0.1 meter is too low for this method. This limit depends on the installed depth of the pressure transmitter.

3.5. Uncertainty Calculated Spectra

A time frame is set in which the mean wave height is calculated for both the signal from the pressure transmitters as the signal from the wave gauges. The time frame contains twelve waves and is set so that any reflection was excluded (the same time frame is used as in Möller et al., 2014). A different time frame is used for every test, as every time frame contains twelve waves. The time frame is set on the basis of wave gauge 2.1. For every pressure transmitter and wave gauge signal the same waves were analysed. To ensure this the group velocity (eq. 14) is used. Several wave gauges were installed at the same location as the pressure transmitters (see table 1). These wave gauges were used to calculate the uncertainty of the calculated spectra. Figures 8a and b show the data obtained from the wave gauges plotted against the data obtained from the pressure transmitters. 2 figures are plotted for both water depths because the tests corresponding to these water depths are treated different in the further analysis. An optimal result is plotted as the line y=x. The coefficient of variation is used to quantify the uncertainty (see appendix E).The uncertainty in the tests over a water depth of 1 meter is 3.23%. The uncertainty in the tests over a water depth of 2 meter is 3.85%. A visual representation of the calculated surface elevation is shown in figure 8c.

Table 3| Model limits due to nonlinear behaviour (tests under dotted line are excluded)

Test	h(m)	T(s)	H(m)
1504	2	2.1	0.2
1803	1	2.1	0.2
1703	2	2.5	0.3
1506	2	2.9	0.2
1702	2	2.9	0.2
1805	1	2.9	0.2
2902	2	2.9	0.4
2102	2	2.9	0.4
2207	1	2.9	0.4
3105	1	2.9	0.4
2504	1	3.3	0.5
1705	2	3.6	0.3
2107	2	3.6	0.6
3110	2	3.6	0.6
2105	2	4.1	0.4
2905	2	4.1	0.4
2402	2	4.1	0.8
3112	2	4.1	0.8
2407	2	4.4	0.9
2506	1	4.6	0.5
2205	2	5.1	0.6
2404	2	5.8	0.8
2502	2	6.2	0.9

4. Data Analysis

In this chapter the analysis of the wave dissipation is discussed and empirical functions on the basis of this analysis are derived. This chapter thus answers research question four and five ('w*hich function could represent the relationship between the average wave height/the average wave energy flux and the distance into the marsh? What is the uncertainty in this function?')*. Paragraph 4.1 discusses the analysis of the wave height dissipation. Paragraph 4.2 is about the analysis of the wave energy flux dissipation. Both paragraphs have the same structure.

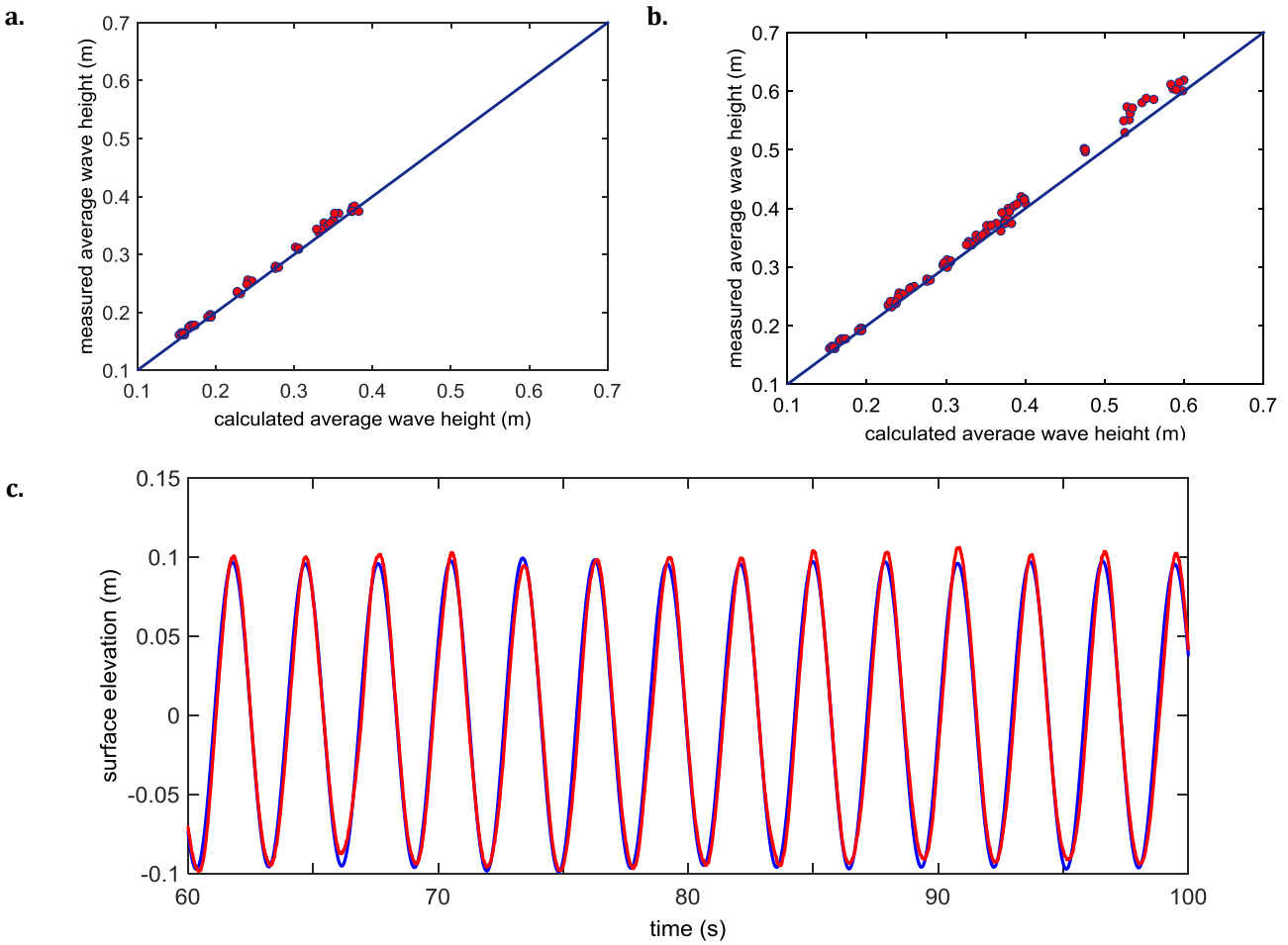

Figure 8| Uncertainty in the calculated surface elevation. a and b, measured (wave gauge signal) and calculated (pressure transmitter signal) wave height corresponding to tests over respectively h(m)=1 and h(m)=2. **c,** signal of WG 2.1 in the used time frame (red) and calculated surface elevation form the signal of PT 2.1 (blue) for test 1506: H(m)=0.2, T(s)=2.9, h(m)=2.

As both theory and research state that wave dissipation can be described as an exponential decay with distance (Dean & Darymple, 1984; Paul & Amos, 2011; Möller et al., 1999; Bouma et al., 2010), at first in both paragraphs an exponential function is introduced. Secondly, the determination of the parameters of this formula is discussed. Thirdly, an analysis of the influence of the water depth is given on the basis of a normalised function. The influence of the water depth partly answers research question six (‘*which parameters influence the evolution of wave dissipation?’).* Fourthly, an answer on research question eight (‘w*hat is the influence of the vegetation?’*) is provided by comparing the parameters obtained from the tests without and with vegetation. Lastly, both paragraphs discuss the uncertainty on the basis of the coefficient of variation (see appendix E).

4.1. Wave Height Dissipation

Exponential Formula

The data is measured with pressure transmitters which are installed at several x-positions. A time frame is set (as discussed in paragraph 3.5) in which the average wave height is calculated for every pressure transmitter. This results in seventeen data points at corresponding x-positions. Matlab is used to fit a line to this data. As both theory and research state that wave height dissipation can be described as an exponential decay with distance (Dean & Darymple, 1984; Paul & Amos, 2011; Möller et al., 1999; Bouma et al., 2010) an exponential function is used for the fit:

$$H_{mean}(x) = a \times e^{bx} \qquad \text{eq. (6)}$$

Where

H_{mean} = average wave height at x-position (m)
a = parameter that describes the initial value of the function
b = parameter that describes the gradient of the

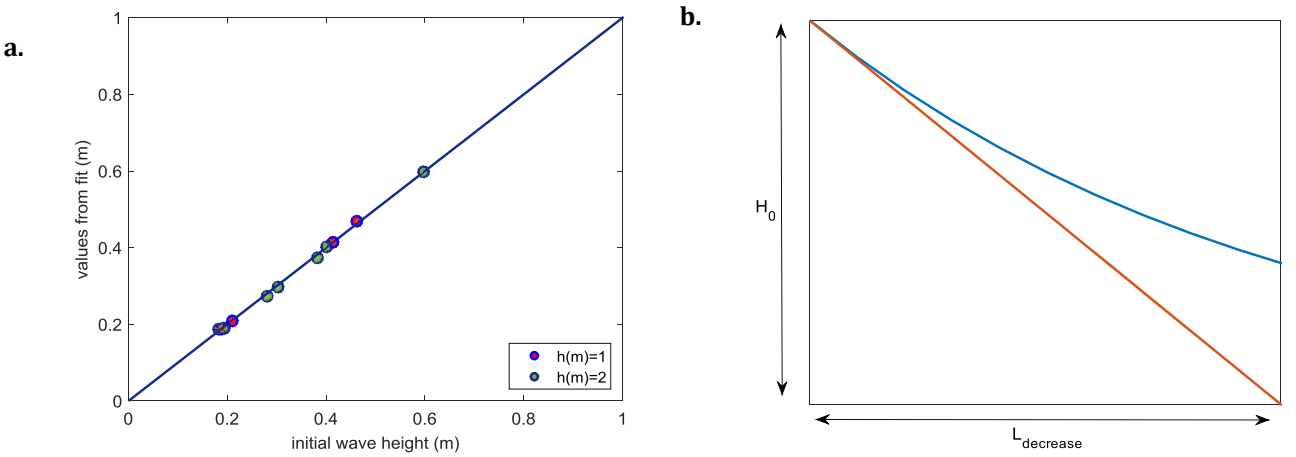

Figure 9| Values for the fitted function. a, obtained values for parameter 'a' from fitted function plotted against the initial wave height. **b,** explanation of the parameters of the empirical function.

function

As parameter 'a' indicates the initial value and parameter 'b' indicates the development of the function the following equation is expected:

$$H_{mean}(x) = H_0 \times e^{b_H x} \qquad \text{eq. (7)}$$

Where

H_0 = the initial wave height measured at PT 2.3 (see table 1) (m)

b_H = decrease parameter which describes the evolution of dissipation (m^{-1})

And $\frac{1}{|b_H|} = L_{decrease}$ ($L_{decrease}$= decrease length) (see figure 9b)

The parameters 'a' and 'b' are obtained for each function. Figure 9a shows that the parameter contained from the fit corresponds to the expected values of the initial wave height. For every test over the vegetated section the parameters and Pearson's correlation coefficients (R) are determined (see appendix D). The average correlation coefficient for tests over a water depth of 1 meter is 0.96525, and over a water depth of 2 meter it is 0.939288. These coefficients thus concern the exponential fits to the data.

Decrease Parameter

Parameter b_H is obtained for every test. Several approaches are tried in order to find a relationship but the behaviour of this parameter only seems to vary over water depth. Therefore 2 different relationships are derived with the use of the average value for b_H:

Average wave height with distance into the salt marsh over a water depth of 1 meter:

$$H_{mean}(x) = H_0 \times e^{-0.0117x} \qquad \text{eq. (8)}$$

Average wave height with distance into the salt marsh over a water depth of 2 meter:

$$H_{mean}(x) = H_0 \times e^{-0.0043x} \qquad \text{eq. (9)}$$

As the tests were only conducted over 2 different water depths it is difficult to derive a relationship on this basis. A suggestion on the basis of a linear relationship is presented in figure 10a. Including this relationship the empirical function can be written as:

Average wave height with distance into the salt marsh:

$$H_{mean}(x) = H_0 \times e^{(0.0074h-0.019)x} \qquad \text{eq. (10)}$$

The relationship predicts that at a water depth of h(m)=2.57 the parameter b_H is zero. This might indicate that at this water depth the influence of vegetation can be neglected. It is also possible that a linear relationship is not correct.

A significantly faster process of wave height dissipation is noticed for the waves over a water depth of 1 meter. This corresponds with the results of Möller et al. (1996). This is visualised in figure 10c on the basis of a normalised equation:

$$\frac{H_{mean(x)}}{H_0} = e^{(0.0074h-0.019)x} \qquad \text{eq. (11)}$$

Note that the term on the left hand side as well as the term on the right hand side is now dimensionless.

The decrease parameter is obtained for every test. The standard deviation in the decrease parameter is respectively 0.0005 m^{-1} and 0.0015 m^{-1} for tests over a water depth of one and two meter. Figure 10c visualises this standard deviation by the dotted lines.

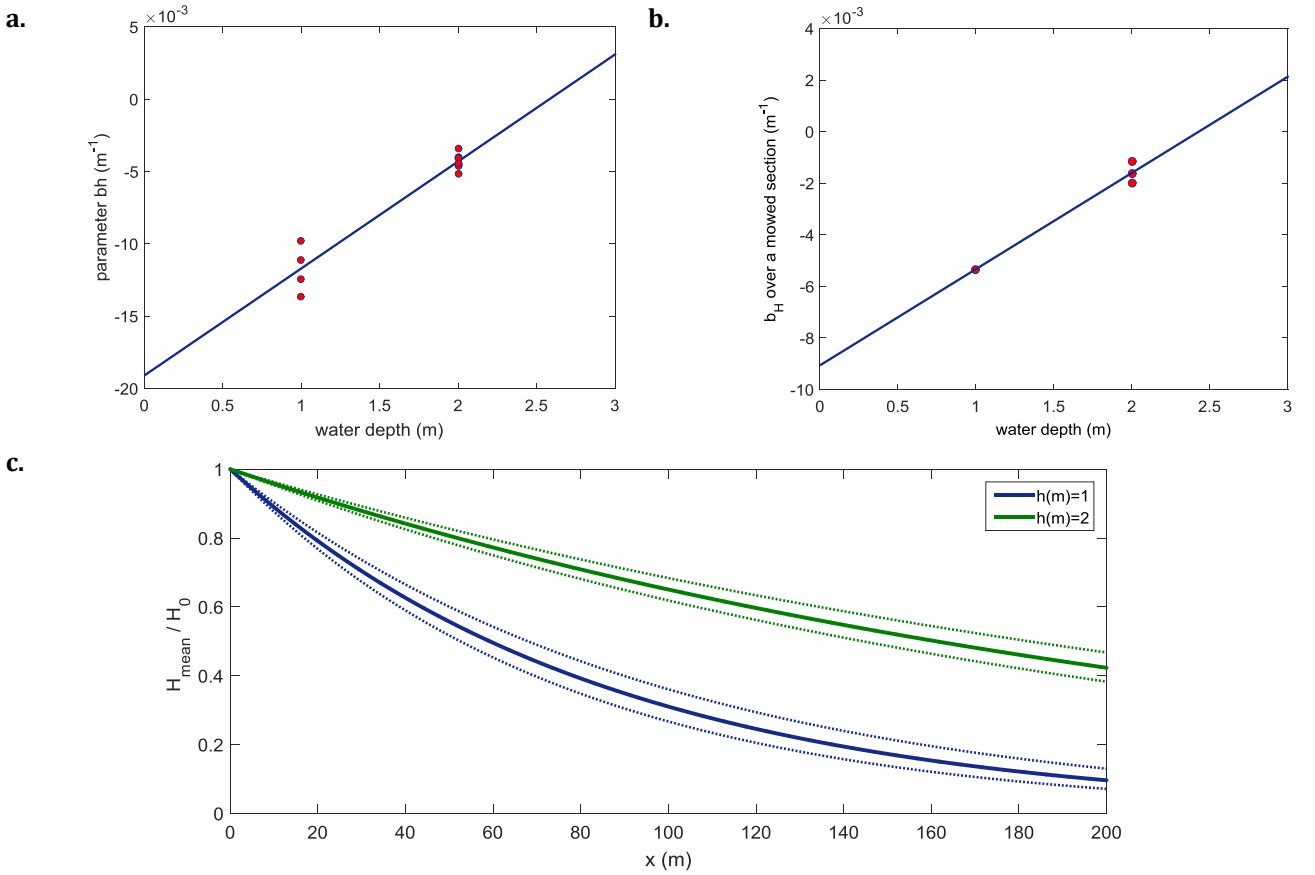

Figure 10| Relationships in the decrease parameter and plots of empirical function. a relationship of the decrease parameter and the water depth red dots are values obtained from the fitted functions). **b,** same as figure 10a but over a mowed section. **c,** plots of equation 11, dotted lines represent the standard deviation in the decrease factor.

Influence of vegetation

For the four tests with mowed vegetated (as listed in table 2) exponential relationships are derived. Using the discussed approach the following relationship is derived:

Average wave height with distance over a mowed section:

$$H_{mean}(x) = H_0 \times e^{(0.0038h - 0.0091)x} \qquad \text{eq. (12)}$$

The decrease parameter as a function of the water depth is plotted in figure 10b. The values for the decrease parameter are closer to zero in comparison with the tests over a vegetated section (compare figure 10a and b). The linear relationship between the decrease parameter and the water depth indicates that the decrease parameters is zero at a water depth of h(m)=2.39. This might indicate that wave dissipation is not influenced by friction from the bottom at this water depth. It might also indicate that a linear relationship is not correct.

A visual representation of the influence of the vegetation is shown in figure 11a, b, c and d. As these figures also contain the data points of the mowed tests it is also a representation of the uncertainty in the derived equation (eq. 12).

Uncertainty

A representation of the uncertainty on the basis of the standard deviation is discussed and shown in figure 10c. Another way of determining the uncertainty is using the coefficient of variation (appendix E). The average wave height derived from the empirical function is plotted against the calculated average wave height (calculated from the pressure data) (see figure 11e and f). The coefficient of variation for tests over a one meter water depth is 9.77%. The coefficient of variation for tests over a two meter water depth is 3.58%. A visual representation of the uncertainty is shown in figure 12 were the calculated average wave height data is plotted against the corresponding empirical functions.

Observation of figure 12 leads to an uncertainty in the derived empirical function as the data points seem to show a linear behaviour. The exponential function might not be correct if extrapolated.

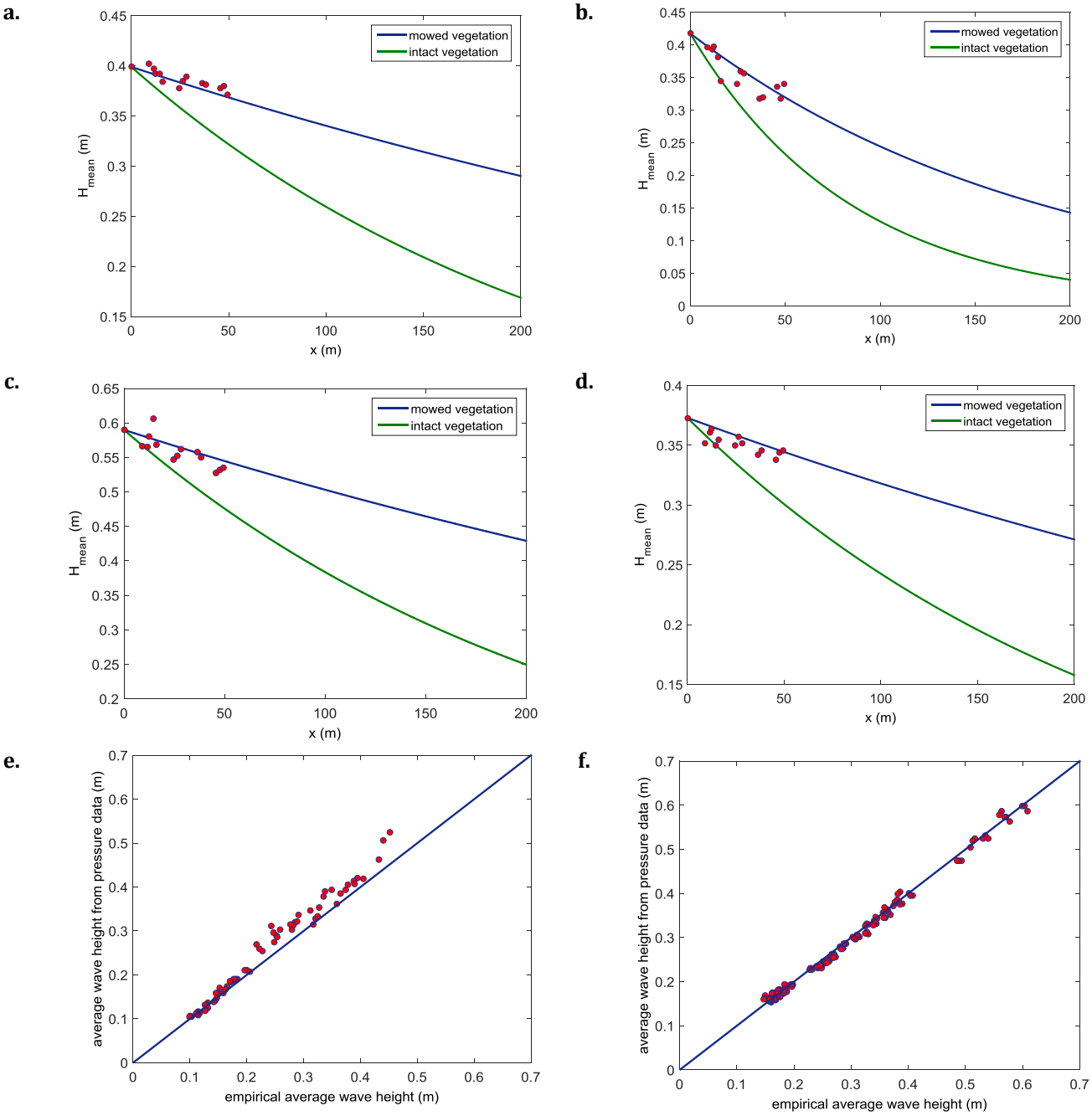

Figure 11| Plots of the empirical functions and visualisation of uncertainty. a, b, c, and d, plots of equation 12 (blue) and equation 10 (green) with the same value for $\mathbf{H_0}$corresponding to the first data point (red). Data points are respectively from test 2902 (h(m)=2, H(m)=0.4, T(s)=2.9), test 2905 (h(m)=2, H(m)=0.4, T(s)=4.1), test 3110 (h(m)=2, H(m)=0.6, T(s)=3.6) and test 3105 (h(m)=1, H(m)=0.4, T(s)=2.9). **e and f,** average wave height obtained from the calculation as presented in chapter 3 plotted against the empirical values for a water depth of respectively 1 and 2 meter.

a.

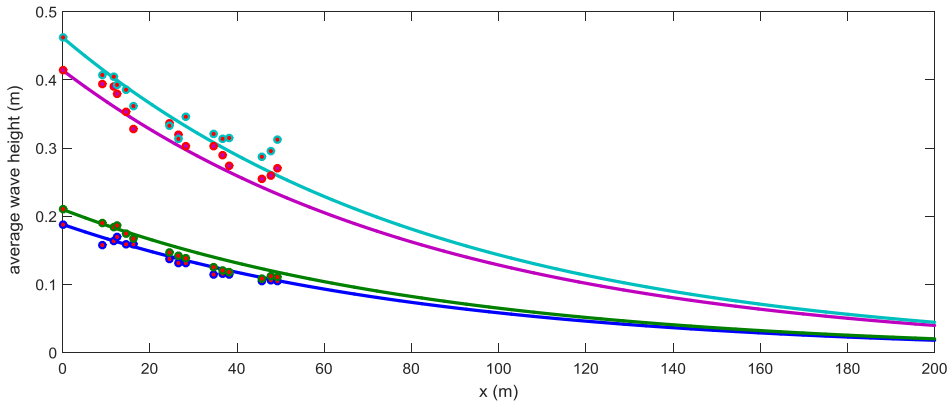

b.

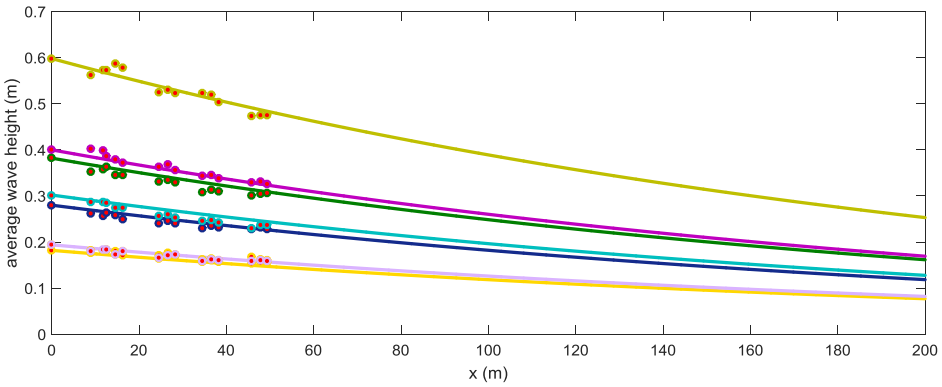

Figure 12| Plots of empirical function as presented in equations 8 and 9. a, plots of equation 8 on the basis of the calculated average wave height for tests over a water depth of 1 meter (red dots). **b,** plots of equation 9 on the basis of the calculated average wave height for tests over a water depth of 2 meter (red dots).

4.2. Wave Energy Flux Dissipation

As the wave energy flux (P) includes wave height, wave period and water depth, this approach is chosen as a second attempt to describe the empirical function. The same approach is followed as explained in paragraph 4.1 only now the mean wave height at every location is used to calculate the wave energy flux at that location.

$$P = E \times C_g \qquad \text{eq. (13)}$$

$$C_g = \frac{1}{2}\left[1 + \frac{4\pi h/\lambda}{\sinh(\frac{4\pi h}{\lambda})}\right]\frac{\lambda}{T} \qquad \text{eq. (14)}$$

$$E = \frac{1}{8}\rho g H^2 \qquad \text{eq. (15)}$$

Where

P = wave energy flux (W/m)
E = mean wave energy density per unit of horizontal area ($J \cdot m^{-2}$)
C_g = group velocity (m/s)
λ = wavelength (m)
ρ = density of liquid (1000 kg· m^{-3})
g = acceleration due to gravity (9.81 m· s^{-2})
T = wave period (s)
h = water depth above marsh surface (m)
H = wave height (m)

Exponential Formula

The wave energy flux is plotted against x for every pressure transmitter. Afterwards an exponential function is fitted. The function is characterised by equation 16.

$$P_{mean}(x) = a \cdot e^{bx} \qquad \text{eq. (16)}$$

Where

$P_{mean}(x)$ = average wave height at a certain distance (m)
a = parameter that describes the initial value of the function
b = parameter that describes the gradient of the function

As parameter 'a' indicates the function value at x=0 and parameter 'b' indicates the development of the function, the following equation is expected:

$$P_{mean}(x) = P_0 \cdot e^{bPx} \qquad \text{eq. (17)}$$

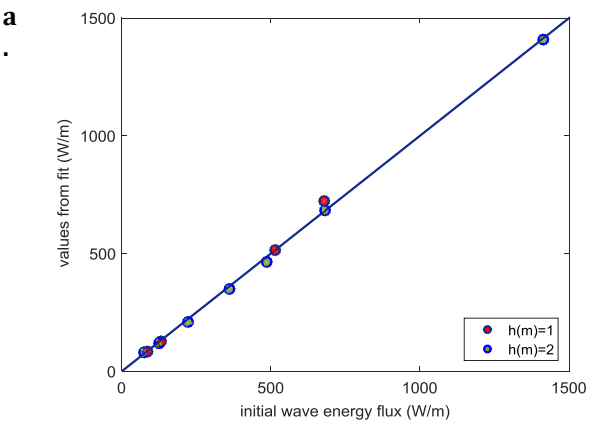

Figure 13| Value for fitted function and relationship in the decrease parameter. a, obtained values for parameter 'a' from fitted function plotted against the initial wave height. **b,** relationship of the decrease parameter and the water depth (red dots are values obtained from the fitted functions).

Where

P_0 = the initial wave energy flux measured at PT 2.3 (see table 1) (W/m)

b_P = decrease parameter which describes the evolution of dissipation (m^{-1})

And $\frac{1}{|b_P|} = L_d$ (L_d= decrease length) (see figure 9b)

The parameters 'a' and 'b' are obtained for each function. Figure 13a shows that the fitted parameter corresponds to the expected values of the initial wave energy flux.

Decrease Parameter

Parameter b_P is obtained for every test. Several approaches are tried in order to find a relationship but the behaviour of this parameter only seems to vary over water depth. Therefore 2 different relationships are derived with the use of the average value for b_P:

Average wave energy flux with distance into the salt marsh over a water depth of 1 meter:

$$P_{mean}(x) = P_0 \times e^{-0.0237x} \quad \text{eq. (18)}$$

Average wave energy flux with distance into the salt marsh over a water depth of 2 meter:

$$P_{mean}(x) = P_0 \times e^{-0.0086x} \quad \text{eq. (19)}$$

Both values for the decrease parameter b_P are approximately two times the value of the decrease parameter b_H (for h(m)=1: $b_P = -0.0237$, $b_H = -0.0117$. for h(m)=2: $b_P = -0.0043$, $b_H = -0.0086$). This indicates the direct relationship between both parameters. The relationship is characterised by equations 13, 14 and 15. Because of this relationship the decrease parameter is not constant in both approaches.

As the tests were only conducted over 2 different water depths it is difficult to derive a relationship. A suggestion on the basis of a linear relationship is presented in figure 13b. Including this relationship the empirical function can be written as:

Average wave height with distance into the salt marsh:

$$P_{mean}(x) = P_0 \times e^{(0.0151h-0.0388)x} \quad \text{eq. (20)}$$

The relationship predicts that at a water depth of h(m)=2.57 the parameter b_P is zero. This might indicate that at this water depth the influence of vegetation can be neglected. It is also possible that a linear relationship is not correct. This value is the same value as derived for b_H which indicates the relationship in both approaches.

A significantly faster process of wave energy flux dissipation is noticed for the waves over a water depth of 1 meter. This is visualised in figure 14a on the basis of a normalised formula:

$$\frac{P_{mean(x)}}{P_0} = e^{(0.0151h-0.0388)x} \quad \text{eq. (21)}$$

Note that the term on the left hand side as well as the term on the right hand side is now dimensionless.

The decrease parameter is obtained for every test. The standard deviation in the decrease parameter is respectively 0.0010 m^{-1} and 0.0026 m^{-1} for tests over a water depth of one and two meter. Figure 14a visualises this standard deviation by the dotted lines.

Influence of vegetation

For the four tests over mowed vegetation (as listed in table 2) exponential relationships are derived. The average wave energy flux (time frame discussed in paragraph 3.5) is calculated for every x-position of the pressure transmitters (table 1). Then an exponential

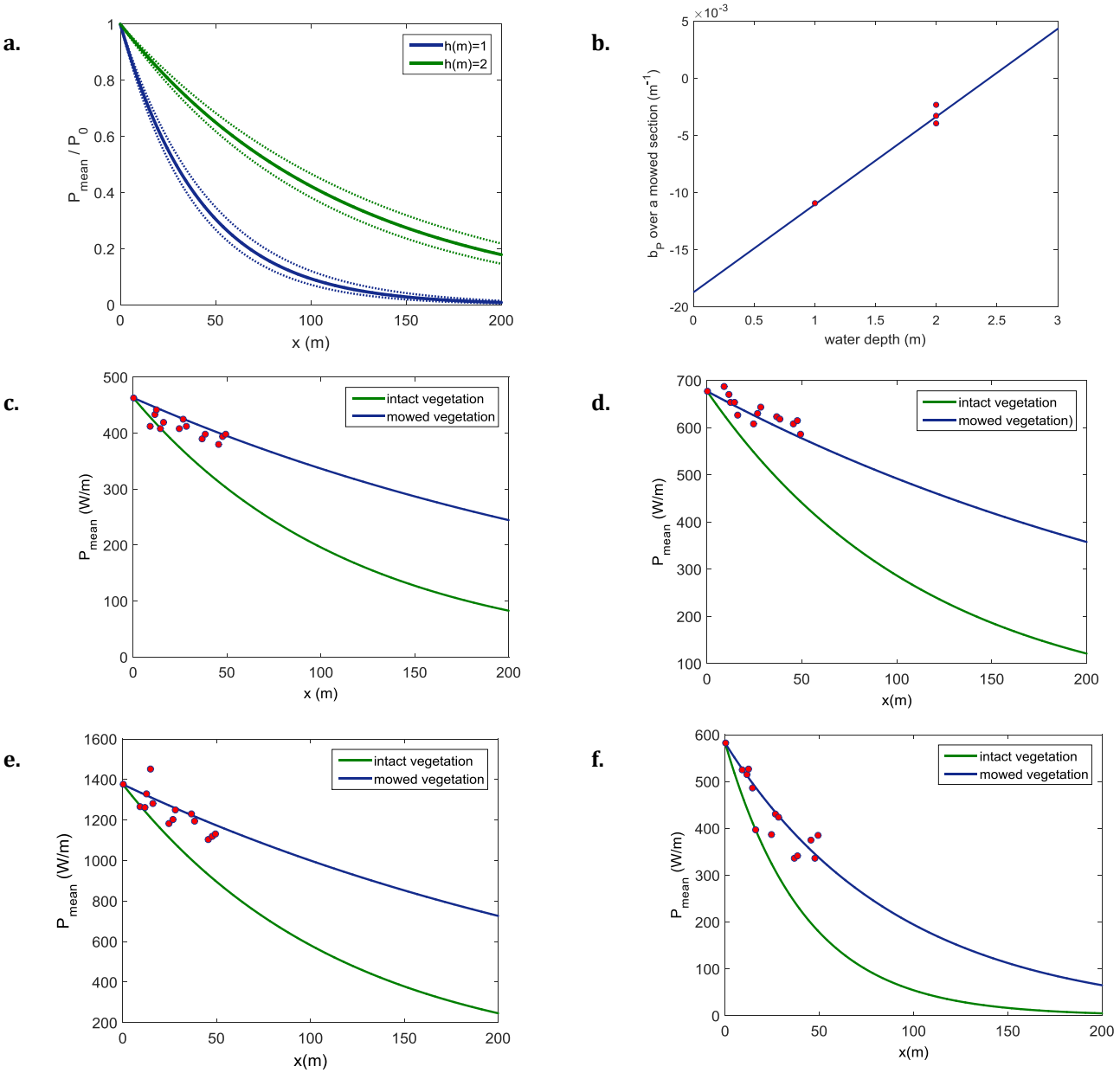

Figure 14| Plots of empirical functions and relationship of the decrease parameter corresponding to a mowed section. a, plots of equation 21, dotted lines represent the standard deviation in the decrease parameter. **b,** relationship of the decrease parameter corresponding to a mowed section and the water depth. **c, d, e and f,** plots of equation 22 (blue) and equation 20 (green) with the same value for H_0 corresponding to the first data point (red). Data points are respectively from test 2902 (h(m)=2, H(m)=0.4, T(s)=2.9), test 2905 (h(m)=2, H(m)=0.4, T(s)=4.1), test 3110 (h(m)=2, H(m)=0.6, T(s)=3.6) and test 3105 (h(m)=1, H(m)=0.4, T(s)=2.9).

function is fitted which describes the relation between the average wave energy flux and x. The following relationship is derived from all fits using the same approach as for the tests over a vegetated section:

Average wave energy flux with distance over a mowed section:

$$P_{mean}(x) = P_0 \times e^{(0.00777h - 0.0187)x} \qquad \text{eq. (22)}$$

The decrease parameter as a function of the water depth is plotted in figure 14b. The values for the decrease parameter are closer to zero in comparison with tests over a vegetated section which indicates a more moderate process of dissipation for the tests over a mowed vegetated section. The linear relationship between the decrease parameter and the water depth indicates that the decrease parameter is zero at a water depth of h(m)=2.41 (compare to paragraph 4.1 where it reaches zero at h(m)=2.39). This might indicate that wave dissipation is not influenced by friction from the bottom at this water depth. It might also indicate that this linear relationship is not correct. A visual representation of the influence of the vegetation is shown in figure 14c,

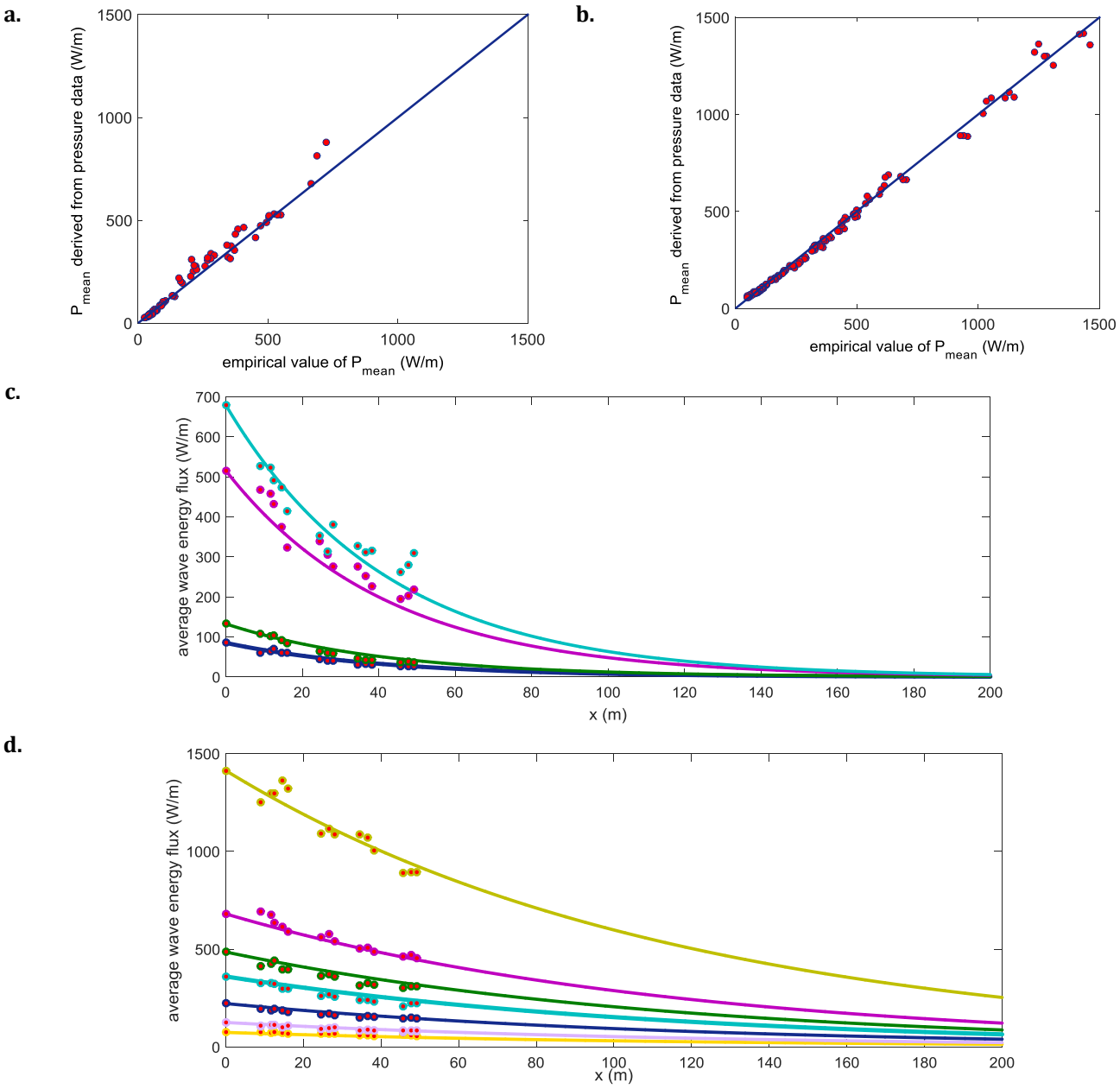

Figure 15| Visualisation of the uncertainty. a and b, average wave energy flux data plotted against the empirical values for a water depth of respectively 1 and 2 meter. **c,** plots of equation 18 on the basis of the calculated average wave energy flux for tests over a water depth of 1 meter (red dots). **d,** plots of equation 19 on the basis of the calculated average wave energy flux for tests over a water depth of 2 meter (red dots).

d, e and f. As these figures also contain the data points of the mowed tests it is also a representation of the uncertainty.

Uncertainty

The uncertainty is determined using the coefficient of variation (appendix E). The average wave height derived from the empirical function is plotted against the calculated average wave height (calculated from the pressure data) (see figure 15a and b). The coefficient of variation for tests over a one meter water depth is 12.60%. The coefficient of variation for tests over a two meter water depth is 7.08%. The uncertainty is thus higher as in the approach on the basis of the wave height (paragraph 4.1). A visual representation of the uncertainty is shown in figure 15c and d were the calculated average wave energy flux data is plotted against the corresponding empirical functions.

Observation of figures … leads to an uncertainty in the derived empirical function as the data points seem to show a linear behaviour. The exponential function might not be correct if extrapolated.

5. DISCUSSION

A critical look to the results is necessary to evaluate their reliability. The data is obtained using pressure transmitters. This data had to be converted to surface elevation in order to do the analysis. A comparison with data from the wave gauges was made in order to verify the accuracy of the calculation. The coefficient of variation for tests over a one meter water depth is 9.77%. The coefficient of variation for tests over a two meter water depth is 3.58%. This difference might have been caused by the applied high and low pass filter. When applying these filters part of the signal is lost. The difference could have also been caused by a calibration error of the pressure transmitters or wave gauges. According to Bishop and Donelan (1987), these errors could be responsible for a considerable part of the discrepancies. The processing of the pressure data into surface elevation is done using linear wave theory. Although this theory seems to be quite exact, it is still an approximation. Nonlinear theory as discussed in Dean and Darymple (1984) might be a better approximation.

Several tests are excluded from the analysis due to their nonlinear behaviour. The applied low pass filter ignores several amplitude peaks of their spectrum.

The 39.44 meter long section appeared to be only the first part of the evolution of dissipation. This explains why the data points seem to follow a linear function. The obtained empirical function might therefore not be extrapolated as has been done in the analysis. Further research over a longer section of vegetation is necessary to verify the results.

The wave period does not seem to influence the evolution of dissipation as the uncertainty in the empirical function derived from only the wave height is lower than the uncertainty of the empirical function derived from the wave energy flux. This is in contrast to the hypothesis. One reason might be that almost no tests were conducted with the same wave height but different wave period. The wave period could also have a negligible influence on the evolution of dissipation.

The decrease parameter as presented in the obtained empirical functions did only show a relationship with the water depth. Therefore different empirical functions are derived for the two water depths. To combine both water depths in one function a linear relationship is suggested. This relationship is based on two data points (two water depths) and is therefore not very reliable. Further research is necessary to verify or discard this relationship.

As the decrease parameter did not show any relationship other than a relationship with the water depth an average value is derived for the empirical functions. However, using the lowest and highest value of this parameter shows a significant difference in the shape of the empirical functions. Further research to this parameter is therefore important.

6. CONCLUSIONS

Q1: Which approach could serve as a method for the transformation from the pressure signal into surface elevation?

Linear wave theory is used as the basis for the method. The calculations are done in frequency domain. A correction factor is applied on the whole spectrum. A high pass filter is used to remove the offset. A low pass filter is necessary as the model considers every frequency component as a single wave. The location of the low pass filter depends on the wave period. After calculating the surface elevation in frequency domain it is transformed into time domain using an inverse fast Fourier transform (IFFT). When compared with the wave gauge signal the calculated surface elevation seems to fit well (see the answer on research question three for quantification), linear theory therefore seems a good approximation. A further elaboration of this research question is to be found in chapter 3.

Q2: What are the limits of this approach?

The signal is measured using pressure transducers. The pressure transducers could not measure a signal of a wave with a wave height of 0.1 meter. This limit depends on the precision of the pressure transducers and on the installed water depth of the pressure transducers. Another limit is noticed at certain nonlinear waves. Some nonlinear wave conditions show amplitude peaks in frequency domain which lay beyond the cut-off frequency. These peaks are therefore ignored. As these peaks are determent for the shape of the waves in time domain the tests are excluded. Not all nonlinear waves show peaks beyond the cut-off frequency. Careful observation is therefore necessary to determine whether a test should be excluded on the basis of this criterion. In the present research the exclusion of tests on the basis of the nonlinearity is presented to be dependent on the wave period and the wave height. A further elaboration of this research question is to be found in paragraph 3.4.

Q3: What is the uncertainty in the calculated surface elevation (from the pressure signal) compared to the signal of the wave gauges?

The uncertainty is separately calculated for both water depths as both water depths show a different behaviour in the further analysis. The uncertainty is calculated using the coefficient of variation (appendix E). The coefficient of variation corresponding to tests over a water depth of 1 meter is 3.23%. The coefficient of variation corresponding to tests over a water depth of 2 meter is 3.85%. A further elaboration of this research question is to be found in paragraph 3.5.

Q4: Which function could represent the relationship between the average wave height and the distance into the marsh? What is the uncertainty in this function?
The following empirical function is derived:

$$H_{mean}(x) = H_0 \times e^{b_H x}$$

$$b_H = 0.0074h - 0.019$$

Where

H_{mean} = average wave height (m)
H_0 = initial wave height (m)
b_H = decrease parameter (m^{-1})
h = water depth (m)

The decrease parameter only showed a relationship with the water depth. As tests were only conducted over two different water depths the presented linear relationship is a suggestion. The uncertainty in this function is measured using the coefficient of variation. The empirical values for H_{mean} are plotted against the calculated values for H_{mean} (calculated from the pressure signal) to determine the coefficient. The coefficient of variation corresponding to tests over a water depth of 1 meter is 9.77%. The coefficient of variation corresponding to tests over a water depth of 2 meter is 3.58%. A further elaboration of this research question is to be found in paragraph 4.1.

Q5: Which function could represent the relationship between the average wave energy flux and the distance into the marsh? What is the uncertainty in this function?
The following empirical function is derived:

$$P_{mean}(x) = P_0 \times e^{b_P x}$$

$$b_P = 0.0151h - 0.0388$$

Where

P_{mean} = average wave energy flux (W/m)
P_0 = initial wave energy flux (W/m)
b_P = decrease parameter (m^{-1})
h = water depth (m)

The decrease parameter only showed a relationship with the water depth. As tests were only conducted over two different water depths the presented linear relationship is a suggestion. The uncertainty in this function is measured using the coefficient of variation. The empirical values for P_{mean} are plotted against the calculated values for P_{mean} (calculated from H_{mean}) to determine this coefficient. The coefficient of variation corresponding to tests over a water depth of 1 meter is 12.60%. The coefficient of variation corresponding to tests over a water depth of 2 meter is 7.08%. A further elaboration of this research question is to be found in paragraph 4.2.

Q6: Which parameters influence the evolution of wave dissipation?
The evolution of wave dissipation is dependent on the decrease parameter. The decrease parameter is presented as a function of the water depth as the water depth significantly influences the evolution of dissipation. A relationship of the decrease parameter to other parameters has not been found. Further research is necessary to determine whether another relationship is possible. An empirical function on the basis of the wave energy flux does not seem to deliver a better relationship than an empirical function only on the basis of the wave height. It seems therefore that the evolution of dissipation is only influenced by the initial wave height and the decrease parameter.

Q7: Which of the approaches as presented in Q4 and Q5 shows the least uncertainty?
For both water depths shows the approach on the basis of the average wave height the least uncertainty. This is in contradiction to the hypothesis. It seems that including wave period and wavelength does not result in a better relationship. Therefore it seems that these parameters do not influence the evolution of wave dissipation. As this is in contradictory to literature (Fonseca & Cahalan, 1992; Moller et al., 1999; Mendez & Losada 2003, Koch et al. 2009) there might be another reason. Further research is necessary to support or discard this conclusion.

Q8: What is the influence of the vegetation?
Möller et al. (2014) concluded that up to 60% of wave height attenuation can be attributed to the salt marsh. Table 4 shows the average decrease parameters for tests over a vegetated section as well as tests over a mowed section. The average decrease parameter for tests over a vegetated section is 2.21 up to 2.87 times higher than the average decrease parameter for tests over a mowed section. A significant influence is thus noticed. The values are derived from the empirical functions as presented in chapter 4.

Table 4| Decrease parameters

	Decrease parameters			
	b_H		b_P	
h(m)	1	2	1	2
Mowed vegetation	−0.0053	−0.0015	−0.0109	−0.0032
Intact vegetation	−0.0117	−0.0043	−0.0237	−0.0086

7. RECOMMENDATIONS

This chapter contains recommendations for further research. At first, an extrapolation of the empirical model describes a process of wave energy dissipation over at least 150 meter. As the test results were obtained from tests in a salt marsh of 39.44 meter the data covers a small part of the total process of dissipation. To provide a more solid basis for the model it is therefore recommended to conduct further research over a longer vegetated section.

Secondly, further research on irregular wave series would benefit the knowledge on the evolution of wave dissipation. Wave spectra are typical for ocean wave conditions. Irregular waves consist of many frequency components but these components do not necessarily lie beyond the applied cut-off frequency as these components all consist of real waves. Therefore the presented method also applies for irregular series. Nevertheless, careful observation to nonlinear behaviour is necessary to determine which wave series to include and which to exclude.

Thirdly, a method is presented in which a low pass filter is not necessary (see paragraph 3.3). In this method the frequency corresponding to the wave period is used for the calculation. Unfortunately using this method an underestimation is noticed in the amplitude peaks of the spectrum. As time is short this approach is not worked out but further research could determine the benefits of this method.

Fourthly, the present research uses a method based on linear theory. Nonlinear wave theory could improve the results.

Fifthly, in the present research the decrease parameter is presented as a function of only the water depth. For this an average value is used. It is possible that the decrease parameter is dependent on other parameters. Further research is necessary to determine this relationship.

Sixthly, the decrease parameter is dependent on the characteristics of the used vegetation. For example shoot density, height of the vegetation and the used plant species are expected to influence the evolution of dissipation. In the present research tests were only conducted over a North Sea marsh community. Further research could determine a relationship of the decrease parameter with specific marsh characteristics.

Seventhly, the empirical function on the basis of the wave height seems to be a better approach than an empirical function on the basis of the wave energy flux. Therefore parameters as the wave period and the wave length do not seem to influence the evolution of dissipation. This is in contrast to the hypothesis. Further research on wave series with the same wave height but different wave periods could determine the influence of the wave period on the evolution of dissipation. An investigation to the behaviour of the group velocity (which includes the wave period and wave length) could answer why the approach on the basis of the wave energy flux shows a higher uncertainty than the approach on the basis of the wave height.

Lastly, in the present research tests were only conducted over two different water depths (one and two meter). The water depth seemed to have a significant influence on the decrease parameter. Therefore a suggestion to include the water depth in the empirical formula is done on the basis of a linear relationship. This relationship is not very reliable as it is only based on two values. Therefore more research with different water depths is necessary to derive a better relationship.

BIBLIOGRAPHY

Koch, E.W., Barbier, E.B., Silliman, B.R., Reed, D.J., Perillo, G.M.E., Hacker, S.D., Granek, E.F., Primavera, J.H., Muthiga, N.,Polasky, S., Halpern, B.S., Kennedy, C.J., Kappel, C.V., & Wolanski, E. (2009). Non-linearity in ecosystem services: temporal and spatial variability in coastal protection. Front Ecol Environ, 7 (1), 29-37.

Bishop, C.T., & Donelan, M.A. (1987). Measuring Waves with Pressure Transmitters. Coastal Engineering, 11, 309-328.

Bouma, T.J., De Vries, M.B., & Herman, M.J. (2010). Comparing ecosystem engineering efficiency of two plant species with contrasting growth strategies. Ecology, 91 (9), 2692-2704.

Möller, I. (2006). Quantifying saltmarsh vegetation and its effect on wave height dissipation: Results from a UK East coast saltmarsh. Estuarine, Coastal and Shelf Science, 69, 337-351.

Paul, M., & Amos, C.L. (2011). Spatial and seasonal variation in wave attenuation over Zostera noltii. Journal of Geophysical Research, 116, 1-16.

Li, Y. & Lin, M. (2012). Regular and irregular wave impacts on floating body. Ocean Engineering, 42, 93-101.

Möller, I., Kudella, M., Rupprecht, F., Spencer, T., Paul, M., Wesenbeeck, B.K., Wolters, G., Jensen, K., Bouma, T.J., Miranda-Lange, M., & Schimmels, S. (2014). Wave attenuation over coastal salt marshes under storm surge conditions. Nature geoscience, 7, 727-731.

Dean, R.G. & Darymple, R.A. (1991). *Water wave mechanics for engineers and scientists.* Singapore: World Scientific Publishing Co. Pte. Ltd.

Möller, I., Spencer, T., Jensen K., Ruprecht, F., Wanner, A., Wesenbeek, B., Wolters, G., Paul, M., Bouma, T., Kudella, M., & Schimmels, S. (2013). Data Storage Report: Wave dissipation and transformation over coastal vegetation under extreme hydrodynamic loading. Hydralab4, HyIV-FZK-07.

Mendez, F. J., & Losada, I. J. (2004). An empirical model to estimate wave propagation of random breaking and nonbreaking waves over vegetation fields. Coastal Engineering, 51, 103-118.

Gedan, K.B., Kirwan, M.L., Wolanski, E., Barbier, E.B., & Silliman, B.R. (2011). The present and future role of coastal wetland vegetation in protecting shorelines: answering recent challenges to the paradigm. Climatic Change, 106, 7-29.

Temmerman, S., De Vries, M.B., & Bouma, T.J. (2012). Coastal marsh die-off and reduced attenuation of coastal floods: A model analysis. Global and Planetary Change, 92-93, 267-274.

APPENDICES

APPENDIX A: LOW PASS FILTER

The table shows the data as obtained using the method as explained in paragraph 3.3.

Table 5| obtained values for the location of the cut-off frequency.

Test	h(m)	T(s)	$H_g(m)$	Location of cut-off frequency (Hz)		
Location obtained from:				**PT 2.1 WG 2.1**	**PT 3.3 WG 3.3**	**PT 4.2 WG 4.2**
1504	2	2.1	0.2	0.08 + 0.48	0.09 + 0.48	
1506	2	2.9	0.2	0.08 + 0.34	0.07 + 0.34	
1702	2	2.9	0.2	0.09 + 0.34	0.08 + 0.34	
1703	2	2.5	0.3	0.09 + 0.40	0.09 + 0.40	
2902	2	2.9	0.4	0.08 + 0.34	0.19 + 0.34	
2102	2	2.9	0.4	0.14 + 0.34	0.18 + 0.34	
1803	1	2.1	0.2	0.09 + 0.48	0.08 + 0.48	
Standardized: 0.08 + frequency corresponding to the wave period						
1705	2	3.6	0.3	0.56	0.56	0.56
2105	2	4.1	0.4	0.53	0.53	0.51
2107	2	3.6	0.6	0.59	0.60	0.58
2205	2	5.1	0.6	0.63	0.60	0.63
2402	2	4.1	0.8	0.56	0.60	0.58
2404	2	5.8	0.8	0.59	0.57	0.67
2407	2	4.4	0.9	0.55	0.61	0.59
2502	2	6.2	0.9	0.65	0.58	0.61
2905	2	4.1	0.4	0.56	0.53	0.55
3110	2	3.6	0.6	0.59	0.59	0.60
3112	2	4.1	0.8	0.56	0.61	0.59
Standardized: 0.51 (minimum value)						
1805	1	2.9	0.2	0.95	0.90	0.65
2207	1	2.9	0.4	0.62	0.65	0.63
2504	1	3.3	0.5	0.89	0.91	0.88
2506	1	4.6	0.5	0.87	0.82	0.71
3105	1	2.9	0.4	0.67	0.65	0.65
Standardized: 0.62 (minimum value)						

APPENDIX B: FREQUENCY CUT TEST 1504

As mentioned in paragraph 3.2 and appendix A, a high and low pass filter are used to remove physical non relevant values. Pressure transmitter 6.2 has an output with a large offset, the low and high pass filter ensure that the calculated surface elevation is physically correct, as the offset is removed.

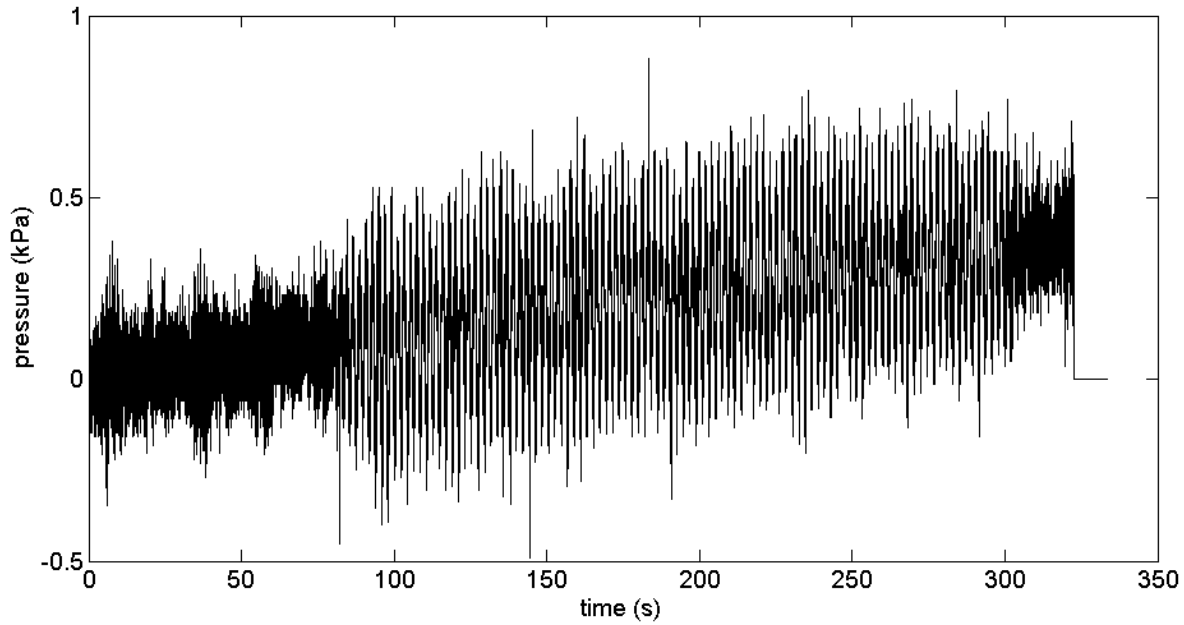

Figure 16| Signal of pressure transmitter PT 6.2 for test 1504 in time domain.

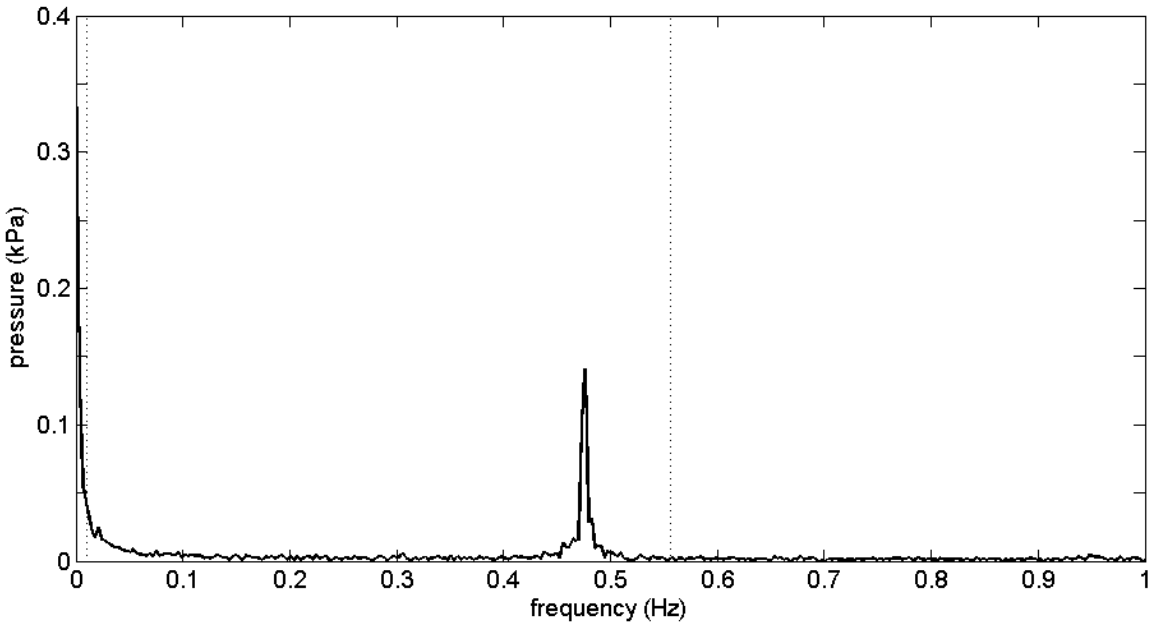

Figure 17| Signal of pressure transmitter PT 6.2 for test 1504 in frequency domain (dashed lines represent cut off frequencies).

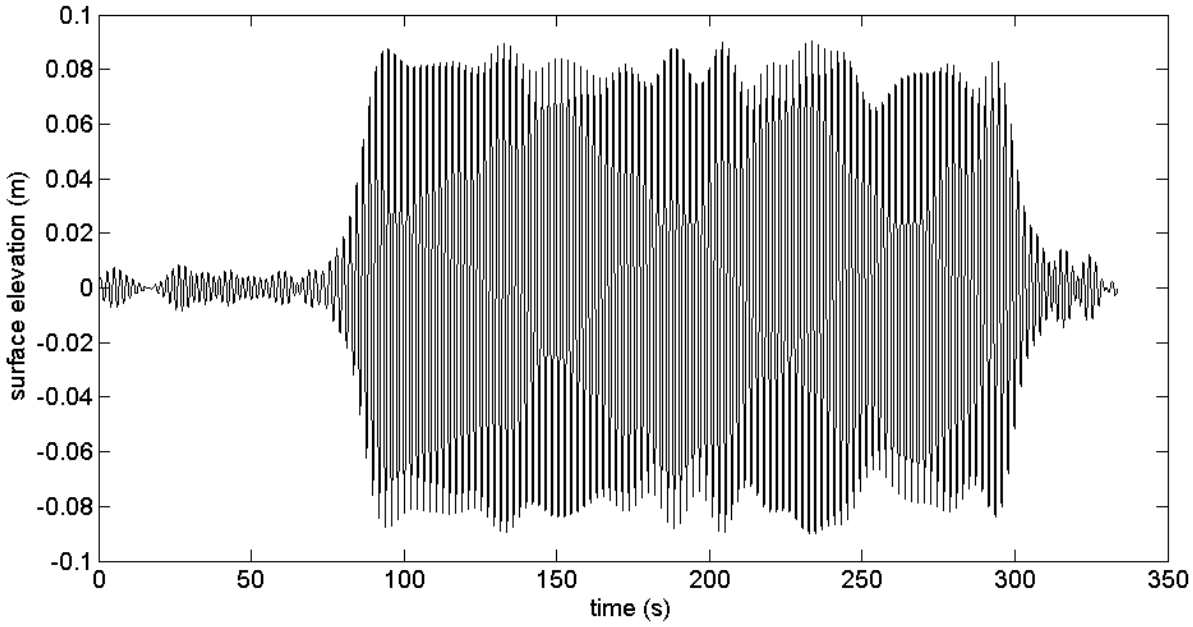

Figure 18| Output of calculations based on the signal of pressure transmitter PT 6.2 for test 1504.

APPENDIX C: EMPIRICAL CORRECTION FACTOR

As discussed in paragraph 3.3 an empirical correction factor is applied. The data corresponding to the described method is presented in this appendix. Note that one value has been excluded due to the significant difference with the other values.

Table 6| Factor N for different tests and different wave gauge-pressure transmitter combinations.

Test	**h(m)**	**T(s)**	$H_s(m)$	**Correction factor**		
Obtained from:				**PT 2.1 WG 2.1**	**PT 3.3 WG 3.3**	**PT 4.2 WG 4.2**
15 04	2	2.1	0.2	0.9697	1.0663	0.9904
15 06	2	2.9	0.2	1.0108	1.0331	1.0238
17 02	2	2.9	0.2	1.0128	1.0295	1.0160
17 03	2	2.5	0.3	1.0167	1.0505	0.9966
29 02	2	2.9	0.4	1.0132	1.0351	1.0167
21 02	2	2.9	0.4	1.0163	1.0407	1.0034
17 05	2	3.6	0.3	1.0133	1.0236	0.9998
21 05	2	4.1	0.4	0.9966	1.0285	1.0044
21 07	2	3.6	0.6	0.9966	1.0101	0.9881
22 05	2	5.1	0.6	1.0151	1.0189	0.9931
24 02	2	4.1	0.8	1.0029	1.0186	0.9950
24 04	2	5.8	0.8	1.0300	0.9909	1.0164
24 07	2	4.4	0.9	0.9893	1.0017	0.9993
25 02	2	6.2	0.9	1.0544	1.0051	1.0125
29 05	2	4.1	0.4	1.0132	~~0.7819~~	1.0233
31 10	2	3.6	0.6	1.0080	0.9957	1.0107
31 12	2	4.1	0.8	1.0088	1.0229	0.9962
18 03	1	2.1	0.2	0.9564	0.9771	1.0040
18 05	1	2.9	0.2	1.0107	0.9797	0.9888
22 07	1	2.9	0.4	1.0252	0.9593	1.0136
25 04	1	3.3	0.5	1.0537	0.9719	0.9677
25 06	1	4.6	0.5	0.9992	0.9741	0.9888
31 05	1	2.9	0.4	1.0607	0.9617	1.0225
					Mean	**1.0079**

APPENDIX D: PEARSON'S CORRELATION COEFFICIENT

For every test over the vegetated section Pearson's correlation coefficient (R) is determined:

$$R = \sqrt{\frac{SSR}{SSE + SSR}} \qquad \text{eq. (23)}$$

$$SSR = \sum_{i=1}^{N} (y_{fit,i} - \overline{y_i})^2 \qquad \text{eq. (24)}$$

$$SSE = \sum_{i=1}^{N} (y_{fit,i} - y_i)^2 \qquad \text{eq. (25)}$$

Where

R	= correlation coefficient
SSR	= sum of squared residuals
SSE	= sum of squared errors
N	= number of data points
$y_{fit,i}$	= value of fitted function
y_i	= value of data
$\overline{y_i}$	= mean value of data

The data points are, dependent on the paragraph, the plotted values of the average wave height (in the time interval) or the plotted values of the average wave energy flux (dependent on the time interval).

APPENDIX E: COEFFICIENT OF VARIATION

The coefficient of variation is used to quantify the uncertainty. The coefficient of variations calculates a relative value:

$$\sigma'_f = \frac{\sigma_f}{\frac{1}{N}\sum f(x_{m,i})} \qquad \text{eq. (26)}$$

$$\sigma_f = \sqrt{\frac{1}{N-1}\sum_{i=1}^{N}\left(P_{m,i} - f(x_{m,i})\right)^2} \qquad \text{eq. (27)}$$

Where

σ'_f	= coefficient of variation (%)
σ_f	= standard deviation (m, W/m)
N	= number of data points (-)
$f(x_{m,i})$	= function value (m, W/m)

In this report the function is always set as the line y=x. The reference data is plotted against the data gained by the empirical function.